Chemistry–A European Journal
Research Article
doi.org/10.1002/chem.202201897
Chemistry Europe
European Chemical Societies Publishing
www.chemeurj.org

In situ *Grignard* Metalation Method, Part II: Scope of the One-Pot Synthesis of Organocalcium Compounds

Philipp Schüler,[a] Simon Sengupta,[a] Alexander Koch,[a] Helmar Görls,[a] Sven Krieck,[a] and Matthias Westerhausen*[a]

Abstract: The in situ *Grignard* Metalation Method (*i*GMM) is a straightforward one-pot strategy to synthesize alkaline-earth metal amides in multi-gram scale with high yields via addition of bromoethane to an ethereal suspension of a primary or secondary amine and magnesium (Part I) or calcium (Part II). This method is highly advantageous because no activation of calcium is required prior to the reaction. Contrary to the magnesium-based *i*GMM, there are some limitations, the most conspicuous one is the large influence of steric factors. The preparation of $Ca(hmds)_2$ succeeds smoothly within a few hours with excellent yields opening the opportunity to prepare large amounts of this reagent. Side reactions and transfer of the *i*GMM to substituted anilines and N-heterocycles as well as other H-acidic substrates such as cyclopentadienes are studied. Bulky amidines cannot be converted directly to calcium amidinates via the *i*GMM but stoichiometric calciation with $Ca(hmds)_2$ enables their preparation.

Introduction

In Part I, the preparation of *Hauser* bases R_2N-MgBr via the in situ *Grignard* metalation method (*i*GMM) has been reported (Scheme 1).[1] This strategy allows a straightforward one-pot synthesis of amidomagnesium halide with high yields on a multi-gram scale by addition of ethyl bromide to an ethereal suspension of magnesium and primary or secondary amine. Occasionally, an operative *Schlenk*-type equilibrium converts heteroleptic R_2N-MgBr into homoleptic $Mg(NR_2)_2$ and $MgBr_2$. Here we studied the transfer of this method to the homologous alkaline-earth metal calcium, which is a globally abundant, environmentally benign and non-toxic alkaline-earth metal. However, its rather inert reaction behavior hinders a widespread application in organic and organometallic chemistry. Calcium has a larger atomization enthalpy than magnesium (Mg: 147.7, Ca 178.2 kJ mol^{-1}) but the lower second ionization potential (Mg: 15.03, Ca: 11.87 eV) facilitating the initial electron transfer from the metal onto organic halides in direct metalation protocols.[2] In addition, oxide layers may cover the metal particles and additionally restrict the chemical reactivity of these alkaline-earth metals.

Scheme 1. Synthesis of *Hauser* bases R_2N-MgBr in an ethereal solvent via the in situ *Grignard* metalation method (*i*GMM). A downstream *Schlenk*-type equilibrium leads to homoleptic $Mg(NR_2)_2$ and $MgBr_2$.

For magnesium the *i*GMM proceeds very well due to the beneficial solvation energy upon coordination of ether bases at magnesium ions. The absolute value of the solvation energy of THF at calcium ions is significantly smaller than found for the harder Mg^{2+} ions.[3] Despite early attempts, the organocalcium chemistry developed more than a century delayed compared to the established magnesium-based *Grignard* chemistry.

The desperate need of soluble calcium-based organometallics has been perturbed by the inertness of the metal itself partly caused by the large atomization energy. To overcome lack of reactivity of the element calcium, many time-consuming and complicated strategies have been developed to activate the metal (distillation,[4] amalgamation,[5] *Rieke*[6] and *Bogdanovic* method,[7] cocondensation of calcium vapor and substrate,[8] thermal decomposition of calcium hydride[9] as well as the ammonia method,[10] i.e. complete removal of ammonia in vacuo from a blue Ca/NH_3 solution). The preparative challenges are discussed exemplary for the synthesis of widely used calcium bis[bis(trimethylsilyl)amide] $Ca(hmds)_2$[11] and of substituted calcocenes $CaCp'_2$.[12]

It has been reported that amines and hexamethyldisilazane H(hmds) reacted with calcium in liquid ammonia or ammonia gas-saturated ethereal and hydrocarbon solutions.[13] In our hands, a rather sluggish reaction mainly yielded solvated and sparingly soluble $Ca(NH_2)_2$ and we were unable to isolate pure

[a] *P. Schüler, S. Sengupta, Dr. A. Koch, Dr. H. Görls, Dr. S. Krieck, Prof. M. Westerhausen*
Institute of Inorganic and Analytical Chemistry
Friedrich Schiller University Jena
Humboldtstraße 8, 07743 Jena (Germany)
E-mail: m.we@uni-jena.de
Homepage: www.westerhausen.uni-jena.de

Supporting information for this article is available on the WWW under https://doi.org/10.1002/chem.202201897

products. The metathetical approach proved to be disadvantageous because an exact stoichiometry had to be ensured. The reaction of two equivalents of K(hmds) with calcium iodide or pseudohalides in ethereal solutions or toluene yielded Ca(hmds)$_2$.[14] However, deficit of K(hmds) gave (pseudo)halide-containing products, excess led to formation of potassium calciates and hence mixtures of Ca(hmds)$_2$ and K[Ca(hmds)$_3$].[15] Therefore, metalation of excess of H(hmds) in hydrocarbons with dibenzylcalcium, which had to be prepared metathetically prior to the synthesis of Ca(hmds)$_2$, was recommended.[15,16] Transmetalation of M(hmds)$_2$ (M=Hg,[17] Sn and Me$_2$Sn[18]) with Ca metal in ethers or toluene offered an alternative access to analytically pure Ca(hmds)$_2$ but the substrates had to be prepared prior to the metal exchange reactions. The reaction of calcium with H(hmds) could be performed in the presence of BiPh$_3$ under ultrasound treatment with an intermediate transmetalation step.[19] Arylcalcium reagents (heavy *Grignard* reagents)[20] are established organometallics that could be used for the metalation of amines.[21] For the synthesis of calcium pyrazolates and bulky amidinates, isolation of intermediately prepared PhCaI was unnecessary and heteroleptic 3,5-diphenylpyrazolyl as well as *N,N'*-dimesitylbenzamidinato calcium iodide were isolated with rather poor yields of 17% and 26%, respectively.[22] Higher yields of homoleptic calcium guanidinates were obtained when calcium was reacted with guanidines in the presence of HgPh$_2$.[23]

All these protocols are related to severe drawbacks such as sophisticated preparative efforts or challenging removal of impurities or toxicity of heavy metal substrates. Therefore, we briefly introduced the *i*GMM as a clean and straightforward method to synthesize multigram amounts of selected calcium amides.[24]

Calcocenes CaCp$_2$ are one of the best studied calcium-based organometallics[12] and many preparative procedures have been developed in the past century such as metalation of cyclopentadiene with calcium and calcium reagents,[13b,c,25] metathesis reaction of CaI$_2$ with KCp,[26] ligand exchange of calcium boranate and NaCp,[27] cocondensation of Ca vapor and CpH,[28] and reaction of PhCaI with KCp followed by a *Schlenk*-type equilibrium.[29] Heteroleptic [(dme)CpCa(μ-Ph)]$_2$ was accessible via the reaction of calcocene with phenyllithium in 1,2-dimethoxyethane (dme).[30] Heteroleptic cyclopentadienylcalcium halides were prepared via a metathetical approach from CaI$_2$ and KCp'[31] and from a mixture of Ca, PhHgBr/Hg and Cp'H.[32] Very recently, quantum chemical calculations verified d-orbital participation at calcium in the bonding of [CaCp$_3$]$^-$ anions,[33] which had been prepared and structurally authenticated earlier as thf adduct [(thf)CaCp$_3$]$^-$.[30]

This brief overview clarifies the importance of straightforward protocols for the syntheses of calcium-based organometallics to advance application of these environmentally beneficial and non-toxic compounds. Here, the scope of the transfer of the in situ *Grignard* metalation method to calcium organometallics has been investigated. In this reaction, a halogenoalkane is added to a suspension of calcium metal and *H*-acidic substrate in an ethereal solvent. More than a century ago, Beckmann described the synthesis of ethylcalcium iodide as a very sparingly soluble compound and stated the necessity of ethereal solvents.[34] Despite several reports thereafter on the synthesis of alkylcalcium halides,[35] the inertness of calcium had been recognized and transmetalation of mercury compounds seemed to be impossible[35c] and the reports on CaMe$_2$ were mistrusted.[36] Due to these challenges, the interest in organocalcium chemistry remained inconstant for several decades. We were unable, too, to refine a high-yield direct synthesis of "simple" alkylcalcium halides via insertion of Ca into an alkyl-halogen bond of halogenoalkanes and at least one trimethylsilyl substituent had to be present to allow an effective synthesis of Me$_3$SiCH$_2$CaX (X=Cl,[37] Br,[37] I[38]). However, CaMe$_2$ is a stable compound and was prepared via ligand exchange between Ca(hmds)$_2$ and MeLi; thereafter, MeCaI was accessible from a *Schlenk*-type equilibrium between CaMe$_2$ and CaI$_2$.[39] A severe drawback of these small heavy *Grignard* reagents is their insolubility in many common organic solvents. Therefore, the *i*GMM seemed to be an advantageous method to avoid large concentrations of alkylcalcium halides on the one hand and to utilize fully the enormous reactivity of alkylcalcium reagents by immediate metalation of *H*-acidic substrates on the other. Calcium and lithium have very similar *Allred-Rochow* electronegativity values of 0.97 and 1.04 whereas magnesium has a significantly larger value of 1.23.[2] The more electropositive character of lithium leads to more polar bonds in lithium amides than found in magnesium-based *Hauser* bases. Thus, Mg(tmp)$_2$ and (tmp)MgBr (tmp = 2,2,6,6-tetramethylpiperidide) were stable in refluxing THF for several hours[40] whereas Li(tmp) decomposed in THF solution already above 0 °C via ether degradation processes.[41] Therefore, we were interested if calcium-based *Hauser* bases could be handled in ethereal solutions.

Results and Discussion

Alkylcalcium halides

The direct synthesis of alkylcalcium compounds via reduction of alkyl halides RX with (activated) calcium was challenging due to side reactions that significantly reduced the yields. On the one hand, *Wurtz*-type coupling reactions led to formation of calcium halides and R–R and on the other, ether degradation lowered the yields and gave impure products. In addition, insolubility led to precipitation of alkylcalcium compounds that could be beneficial because the calcium organometallics were withdrawn from the reaction mixtures and protected by this way but at the same time, this behavior prevented homogeneous reaction conditions.

We reinvestigated the direct synthesis of alkylcalcium compounds (Table 1). Methyl (entries 1 to 3), ethyl (entries 4 to 8) and isopropyl iodide (entries 9 and 10) were reduced with slight excess of calcium in THF. During the reaction an insoluble precipitate formed which contained excess calcium, calcium halides and probably also alkylcalcium compounds. After the given reaction time, an aliquot of the supernatant clear reaction

Table 1. Screening of reaction conditions to identify the optimal procedure for the synthesis of alkylcalcium iodide via the reduction of iodoalkane with calcium.

Entry	R	Ca[a]	Temp. [°C]	Reaction time [h]	Conversion rate [%]
1	Me	Ca*	−78	2	25
2	Me	Ca*	−78	4	21
3	Me	Ca*	−78→10	15	12
4	Et	Ca*	−78	6	20
5	Et	Ca*	−78	3	20
6	Et	Ca*	−78	3	8[b]
7	Et	Ca	−78	3	2
8	Et	Ca*	−78→30	4	16
9	*i*Pr	Ca*	r.t.	3	0[c]
10	*i*Pr	Ca*	−78→30	5	3

[a] The star denotes activated calcium powder obtained by complete removal of NH_3 from ammonia-calcium solutions whereas in entry 7 commercially purchased Ca was used. [b] Synthesis in an unstirred reaction mixture. [c] At room temperature, a fast *Wurtz*-type coupling occurred yielding hexane but no *i*PrCaI was detected.

solution was hydrolized and titrated with sulfuric acid to determine the alkalinity for elucidation of the conversion rate.

A conversion of 25% was obtained for methyl iodide for a reaction period of 2 h at −78 °C (entry 1). A longer reaction time reduced the yield (entry 2) as did a higher temperature (entry 3). A similar finding was observed for ethyl iodide, but the degradation was slower and after 6 h, still a conversion of 20% was determined (entry 4). Working in a stirred solution is highly beneficial to enhance the conversion rate (entries 5 and 6). In all these experiments, activated calcium powder had been used. Without activation the reactivity of calcium metal decreased significantly (entry 7). As observed for methyl iodide, higher temperatures reduced the yield of organocalcium compounds (entry 8). In contrast to this finding, traces of isopropylcalcium compounds formed at lower temperatures (entry 10) whereas at room temperature no formation to alkylcalcium compounds had been found but a very fast and dominating *Wurtz*-type coupling reaction (entry 9).

Analogously to the classical *Grignard* reagents a *Schlenk*-type equilibrium is operative in THF interconverting heteroleptic RCaI into the homoleptic complexes CaR_2 and CaI_2 as depicted in Scheme 2.

In a THF solution of MeCaI the resonances of the methyl groups were observed at high field allowing an assignment to MeCaI and $CaMe_2$ at $\delta = -1.21$ and -1.37 ppm, respectively. At room temperature the *Schlenk*-type equilibrium is strongly shifted in favor of the heteroleptic compound as shown in Figure 1.

The direct synthesis of methyl and ethyl iodide with activated calcium in diethyl ether gave much precipitate, presumably alkylcalcium compounds besides calcium bromide.

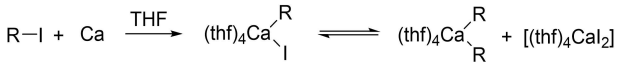

Scheme 2. Synthesis of alkylcalcium iodides in THF solution (see text and Table 1).

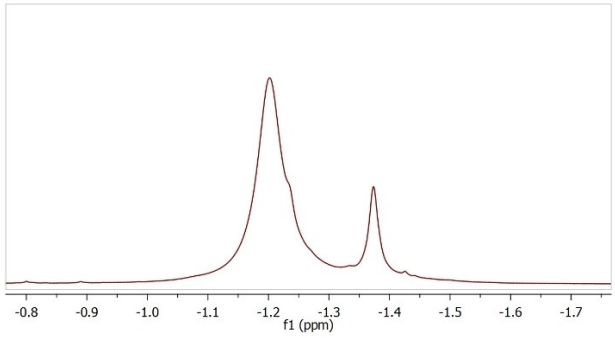

Figure 1. 1H NMR spectrum (400 MHz, THF/[D_8]THF) of the reduction of MeI with Ca in THF at room temperature showing MeCaI and $CaMe_2$ at $\delta = -1.21$ and -1.37 ppm, respectively, due to an operative *Schlenk*-type equilibrium.

The supernatant solution contained no organocalcium derivatives due to the insolubility of the organocalcium complexes in this solvent. Addition of benzaldehyde to the suspension of ethylcalcium compounds in diethyl ether led to formation of the addition product with a yield of 65% which is in agreement with earlier reports.[35]

Reaction conditions of the iGMM

To begin with this study, we identified the ideal solvent for the *i*GMM. The benchmark reaction was the synthesis of calcium bis[bis(trimethylsilyl)amide] $Ca(hmds)_2$ via addition of ethyl bromide to a suspension of commercial calcium turnings (without activation) and hexamethyldisilazane H(hmds) with a strictly equimolar ratio as depicted in Scheme 3. The *Schlenk*-type equilibrium converted the heteroleptic complex $(L)_nCa(hmds)Br$ quantitatively into the homoleptic congeners $(L)_nCa(hmds)_2$ and $(L)_nCaBr_2$. We chose ethyl bromide instead of ethyl iodide to enable the procedure of the *i*GMM at room temperature. The usage of EtI required very low reaction temperatures to suppress the dominating *Wurtz*-type coupling reaction.

In THF the conversion rate was 46% (Table 2, entry 1) after 2 h reaction time. In this case, intermediately formed ethylcalcium bromide reacted with nearly half of H(hmds) to the amides. Competing *Wurtz*-type coupling reactions also led to formation of butane and calcium bromide. In all other investigated solvents, the conversion rate was significantly lower or no conversion at all was found. Surprisingly, 2-methyltetrahydrofuran was an unsuitable solvent (entry 2). In diethyl ether (entry 8) no reaction between calcium and ethyl

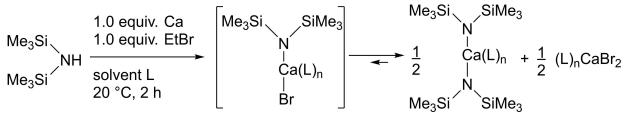

Scheme 3. The benchmark reaction for testing of the suitability of diverse solvents L for the *i*GMM. *Lewis* basic solvents L may act as ligands at the metal ions.

Table 2. Screening of solvents for the preparation of $Ca(hmds)_2$ via the *i*GMM as depicted in Scheme 2 (see text).

Entry	Solvent[a] L	Alkalinity[b] [%]
1	THF	46
2	2-MeTHF	0
3	1,3-Dioxolane	0
4	Methylal	0
5	CPME	0
6	Toluene	0
7	DME	17
8	Et_2O	0

[a] Solvents: THF – tetrahydrofuran, 2-Me-THF – 2-methyltetrahydrofuran, Methylal – 1,1-dimethoxymethane, CPME – cyclopentylmethylether, DME – 1,2-dimethoxyethane, Et_2O – diethyl ether. [b] Reaction was performed using an exact 1.0:1.0 stoichiometry for Ca:EtBr and an aliquot was titrated after 2 h reaction time.

bromide was observed. Bidentate 1,2-dimethoxyethane (DME, entry 7) gave a low conversion rate. Steric hindrance (entry 2) and low basicity of the solvents (entries 3–6 and 8) proved to be highly disadvantageous.

The preparation of calcium-based *Hauser* bases proceeded smoothly in THF at room temperature. To determine optimal reaction time and temperature, the benchmark reaction was repeated at different temperatures between −40 °C and +40 °C (Figure 2). At −40 °C no reaction occurred. Increasing temperature up to 20 °C accelerated conversion and formation of calcium amide. Higher temperatures were disadvantageous and lower rates of amide formation were observed due to accelerated degradation reactions (ether cleavage) and enhanced amounts of *Wurtz*-type coupling products.

To investigate competing *i*GMM and *Wurtz*-type coupling reactions, we used benzyl bromide BnBr instead of ethyl bromide to trigger the formation of $Ca(hmds)_2$ in THF according to Scheme 3 to avoid the formation of volatile and gaseous products. In the benchmark reaction for the synthesis of solvated $Ca(hmds)_2$ the substrates were present with a molar ratio of 1.0:1.0:1.0 for H(hmds):BnBr:Ca. To elucidate the influence of excess and deficit of one of the components, the concentration of only one of the substrates was varied whereas the amount of the two other components remained unchanged (Figure 3). The conversion was monitored after 2 h by ^{1}H NMR spectroscopy. Benzyl bromide was unreacted substrate, toluene the product of the *i*GMM and 1,2-diphenylethane the side product of the competing *Wurtz*-type coupling reaction. For the benchmark reaction with the ideal substrate ratio of 1.0:1.0:1.0 for H(hmds):BnBr:Ca approx. 70% of toluene and 30% of 1,2-diphenylethane were found which verifies the dominating *i*GMM and minor *Wurtz*-type side reactions. Expectedly, deficit of H(hmds) promoted the *Wurtz*-type reaction and hence formation of 1,2-diphenylethane. Surprisingly, the presence of only a very small amount of H(hmds) decelerated the formation of the initial heavy *Grignard* reagent BnCaBr and unreacted BnBr was still present. Deficit of BnBr led to slightly enhanced toluene concentrations whereas an excess of BnBr was highly disadvantageous facilitating the *Wurtz*-type coupling reaction and in addition, unreacted BnBr remained in solution due to the constant amount of calcium. Similarly, reduction of the amount of calcium led to excess of benzyl bromide. In summary, an equimolar ratio of H(hmds) and calcium is beneficial whereas a slight deficit of BnBr was advantageous.

A common side reaction of alkyl- and arylcalcium compounds is ether degradation, leading to formation of ethene and calcium vinylate.[20] However, ether degradation processes became negligible during the preparation of $[(thf)_2Ca(hmds)_2]$ by this *i*GMM because large concentrations of organocalcium reagents are avoided in these reaction mixtures due to the fast reaction of these reagents with *H*-acidic substrates.

Nevertheless, very minor amounts of ethene formed during the synthesis of $Ca(hmds)_2$ via the *i*GMM. On the surface of the metal particles, ethene formed from ethyl moieties. This finding had been verified by a similar procedure in $[D_8]$THF and no deuterated ethene species were detected excluding significant THF degradation processes.

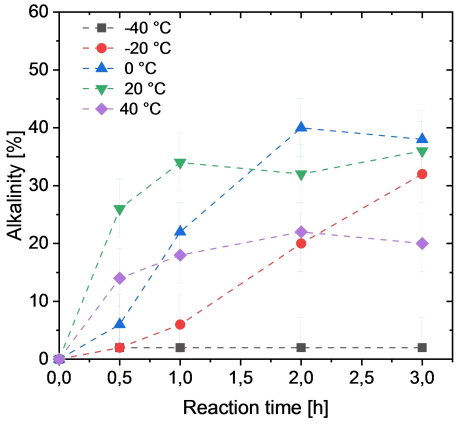

Figure 2. Progress of the reaction of H(hmds) with calcium metal after addition of ethyl bromide in THF in dependency of the reaction time.

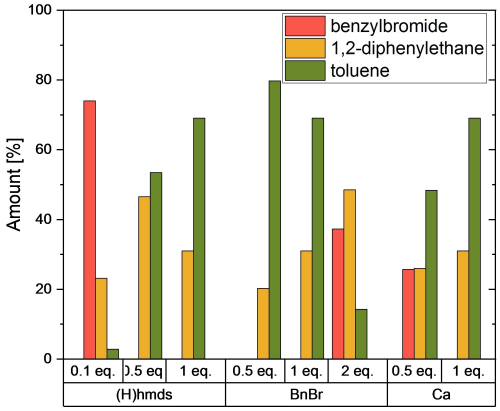

Figure 3. Formation of toluene (green, *i*GMM product) and 1,2-diphenylethane (yellow, *Wurtz*-type coupling product) monitored after a reaction time of 2 h between calcium and H(hmds) after addition of benzyl bromide (red, unconsumed starting material). The bottom line gives the substrates of which the number of equivalents (abbreviated as eq.) has been varied whereas exactly 1.0 equivalent of the other two components have been retained.

Substrate screening

For substrate screening, the reactions were performed in THF as depicted in Scheme 4. One equivalent of EtBr was added to a suspension of Ca and amine in THF at room temperature. Again, the *Schlenk*-type equilibrium was strongly shifted toward the homoleptic complexes. This had been observed earlier for the tmeda adducts of diisopropylamide and tetramethylpiperidide which were prepared via a metathetical approach of KNR_2 and CaI_2 and regardless of the applied stoichiometry, the homoleptic calcium bis(amides) had been observed exclusively;[42] homoleptic [(tmeda)Ca(tmp)$_2$] was also accessible by metalation of H(tmp) with dibenzylcalcium.[43]

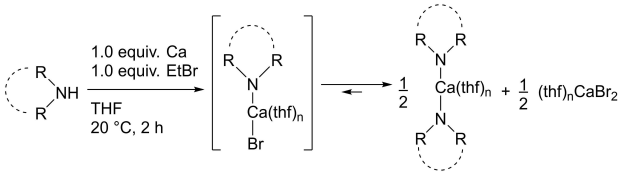

Scheme 4. Substrate screening for the *i*GMM in THF at 20 °C with subsequent *Schlenk*-type equilibrium converting heteroleptic into homoleptic complexes (see text and Scheme 3).

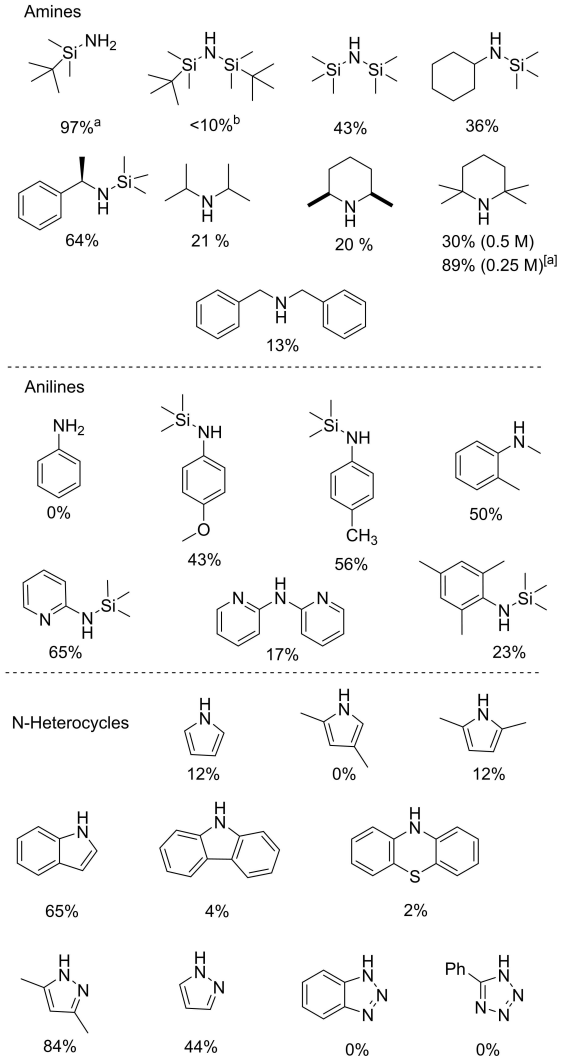

Scheme 5. Substrate screening with NH acidic compounds (top: amines, in the middle: substituted anilines, bottom: N-heterocycles) and yields for the *i*GMM (see text and Scheme 3) using 0.5 M amine solutions. For tetramethylpiperidine, the yield could be enhanced applying diluted solutions (marked with [a]).

In Scheme 5, the outcome of the *i*GMM was investigated for diverse substrates at room temperature with a strict 1.0:1.0:1.0 molar ratio for amine:EtBr:Ca and a reaction time of 2 h. The applied amines can be divided into three groups, namely amines, anilines and N-heterocycles. Trialkylsilyl substituents were beneficial for the *i*GMM if only moderate steric hindrance was introduced. Dialkylamines could be prepared by this method in moderate yields, however, working in diluted solutions is advantageous to avoid precipitate and coverage of the calcium particles as had been studied for the conversion of 2,2,6,6-tetramethylpiperidine.

Surprisingly, aniline was inert under these reaction conditions, but activation of the N–H functionality by trialkylsilyl substituents enabled the conversion to anilides. *N*-Methylaniline was a suitable substrate, too. Bulky mesityl groups decelerated the conversion and hence reduced the yields. Pyrroles generally gave low conversion rates with indole being an exception. Pyrazoles were suitable substrates and high yields were obtained for 3,5-dimethylpyrazole. Larger numbers of nitrogen atoms in the heterocycle were highly disadvantage and no conversion was observed for triazoles and tetrazoles containing benzo and phenyl moieties. In addition, calciation of *N,N′*-diarylformamidines and *N,N′*-bis(2,6-diisopropylphenyl)-β-diketimines was impossible via the *i*GMM which can be explained by steric shielding of the reactive N–H functionality. The acidity of the N–H group allowed straightforward metalation with Ca(hmds)$_2$ in ethereal solvents verifying an adequate acidity as depicted in Scheme 6. In summary, sufficient *Brønsted* acidic character was compulsory and only low to moderate steric shielding of the H-acidic functionality was tolerated. These requirements underline that the reaction is kinetically controlled and accessibility of the H-acidic site is mandatory for successful competition with side reactions such as *Wurtz*-type coupling reactions and ether degradation processes.

An overview on the proposed reaction scheme as well as possible side reactions is depicted in Scheme 7.

The electron transfer from the calcium particle onto bromoethane yields a radical anion which dissociates into a bromide

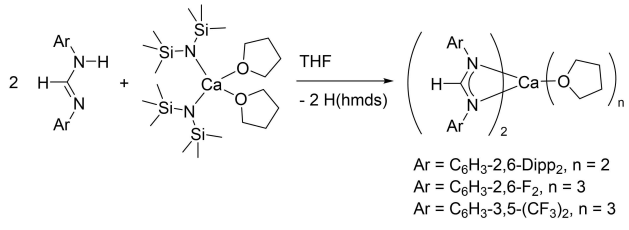

Scheme 6. Calciation of *N,N′*-diarylformamidines with Ca(hmds)$_2$ in THF yielding the corresponding calcium bis(formamidinates).

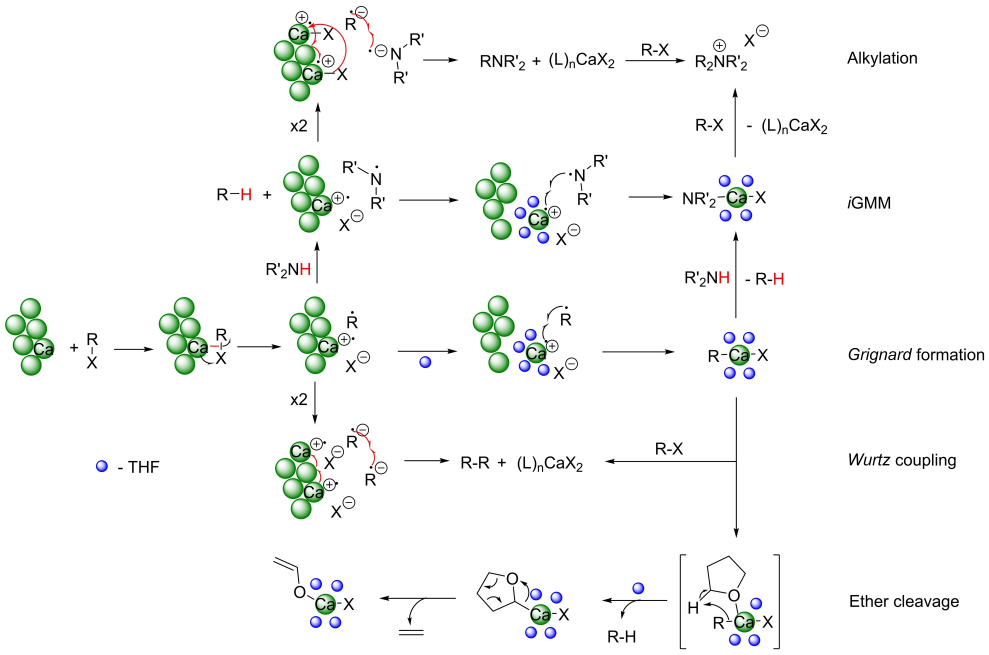

Scheme 7. Proposed reaction diagram of the in situ *Grignard* metalation method in ethereal solvents like THF using calcium particles. *Grignard* reagent formation and iGMM represent the requested reactions whereas *Wurtz*-type coupling reactions and ether degradation are undesired competing processes. In most cases, alkylation reactions are negligible side reactions. Increasing steric hindrance of the H-acidic site favor the *Wurtz*-type side reaction.

ion and an ethyl radical. Recombination of these species leads to EtCaBr in analogy to the *Grignard* reaction. This heavy *Grignard* reagent is highly reactive and can (i) degrade ethereal solvent, (ii) react with another equivalent of EtBr (*Wurtz*-type coupling and formation of butane) or (iii) undergo the projected deprotonation of H-acidic substrates. Ether cleavage is a slow and hence minor side reaction whereas *Wurtz*-type coupling and calciation of H-acidic substrates often compete. Low temperatures accelerate *Wurtz*-type coupling reactions as has been demonstrated in the absence of amines whereas temperatures above room temperature enhance ether degradation side reactions. Despite these limitations with respect to reaction conditions (especially solvent and reaction temperature) the enormous advantage of the *i*GMM is the avoidance of large concentrations of highly reactive EtCaBr. During the *i*GMM, the calcium particles dissolve and therefore, this reaction is limited to soluble organocalcium compounds, otherwise the product precipitates on the particle surface and the reaction ceases. On the one hand, substitution of the H-acidic substrates may be mandatory to enhance solubility in THF but on the other hand very bulky groups hinder access of EtCaBr at the H-acidic functionality limiting general application of the *i*GMM.

Transfer of the *i*GMM to CH-acidic substrates was included in this study. Thus, cyclopentadienes, phenyl-substituted methane, fluorene derivatives, indene and methylsulfonylbenzene were included in our investigation (Scheme 8). The synthesis of cyclopentadienides succeeded via the *i*GMM whereas decreasing yields were obtained with increasing bulkiness of the substituted cyclopentadienes. Toluene was inert in this reaction but diphenylmethane gave low yields of diphenylmethanide; this substance class had been prepared earlier via a metathetical approach.[44,45] A third phenyl group was disadvantageous in this procedure but bis(triphenylmethyl)calcium had also been synthesized earlier.[45,46] Indene and fluorene derivatives were unsuitable substrates even though, 9-trimethylsilylfluorene showed low conversion rates. Again, steric bulk was obstructive to achieve high conversion rates via the *i*GMM.

The *i*GMM of (substituted) cyclopentadienes yielded intermediate cyclopentadienylcalcium bromides that underwent a *Schlenk*-type equilibrium yielding homoleptic calcocenes and calcium bromide as depicted in Scheme 9. In addition, heteroleptic Cp^RCaBr showed an aggregation-deaggregation equilibrium as had been verified by DOSY NMR spectroscopy.

To investigate the exchange equilibrium between homo- and heteroleptic species and to avoid interfering aggregation processes, a 1:1 mixture of $[(thf)_2CaCp_2]$ and $[(thf)_2Ca(hmds)_2]$ was investigated in $[D_8]$THF solution by NMR spectroscopy as depicted in Scheme 10.

The singlets of the Cp and hmds ligands are clearly separated and integration of these resonances allowed the determination of the equilibrium constant K in dependency of the temperature T. Graphical analysis (Figure 4) enabled the elucidation of the thermodynamic parameters for this exothermic reaction with the following values at a 0.1 M solution: $\Delta H = -11.2 \pm 1.0\ kJ\,mol^{-1}$ and $\Delta S = 39.5 \pm 3.3\ J\,mol^{-1}\,K^{-1}$. Dilution and, of course, temperature influence the equilibrium constant of the ligand exchange.

The exchange rates were determined by ^1H EXSY NMR spectroscopy depending on the temperature as shown in Figure 5. In this kinetic study, the values for the transition state were elucidated as $\Delta H^{\#} = 38.7 \pm 2.2\ kJ\,mol^{-1}$ and $\Delta S^{\#} = 316.5 \pm$

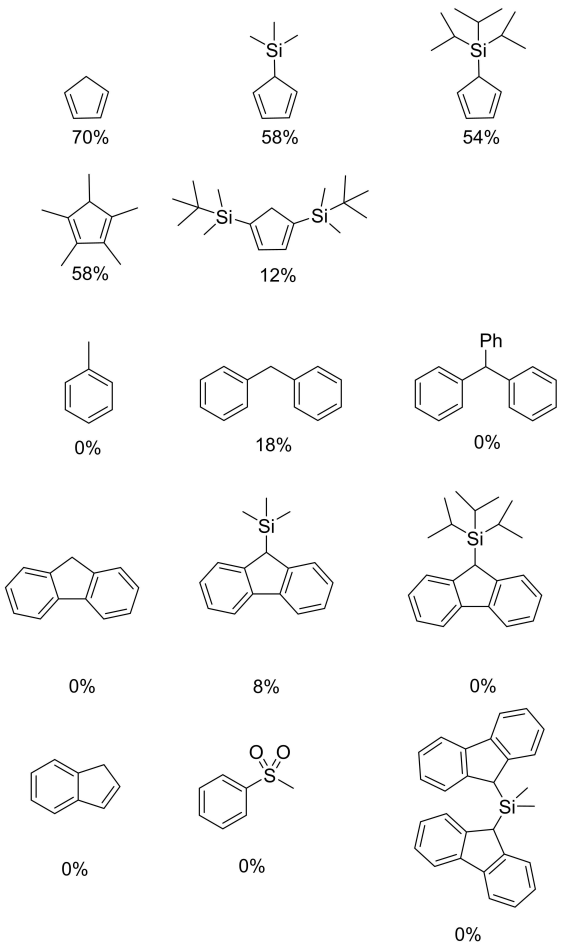

Scheme 8. Substrate screening with CH acidic compounds derived from cyclopentadiene and yields for the *i*GMM (see text).

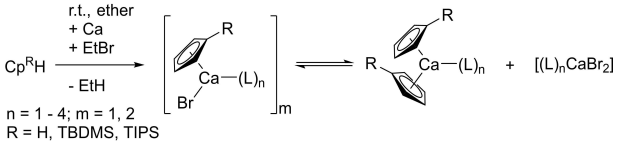

Scheme 9. Synthesis of heteroleptic cyclopentadienylcalcium bromide and subsequent *Schlenk*-type equilibrium yielding homoleptic calcocenes and calcium bromide (TBDMS tert-butyldimethylsilyl, TIPS triisopropylsilyl).

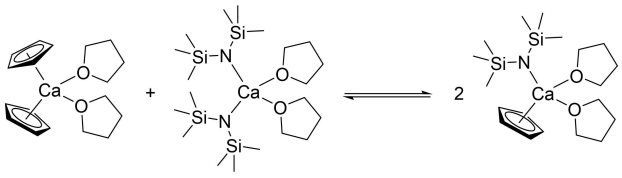

Scheme 10. Equilibrium between homoleptic calcocene and $Ca(hmds)_2$ on the one side and heteroleptic CpCa(hmds) on the other in $[D_8]$THF.

6.4 J mol^{-1} K^{-1}. We interpret the large entropy value by a dissociative mechanism, i.e. dissociation of the calcocene into $[CpCa]^+$ cations and Cp^- anions, and hence an enhancement of

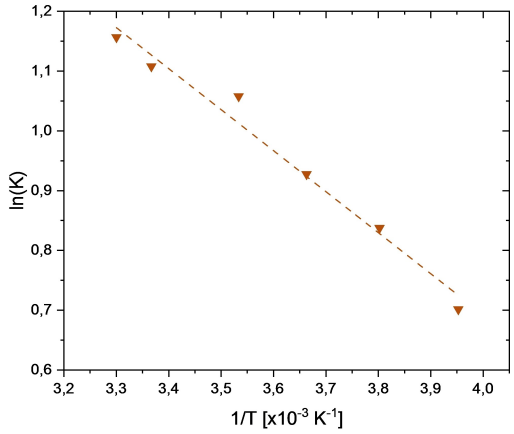

Figure 4. Presentation of the dependency of the equilibrium constant K as ln(K) for the reaction of calcocene with $Ca(hmds)_2$ in $[D_8]$THF (see Scheme 9) from the temperature outlined as T^{-1} for the elucidation of the thermodynamic parameters ΔH and ΔS (see text).

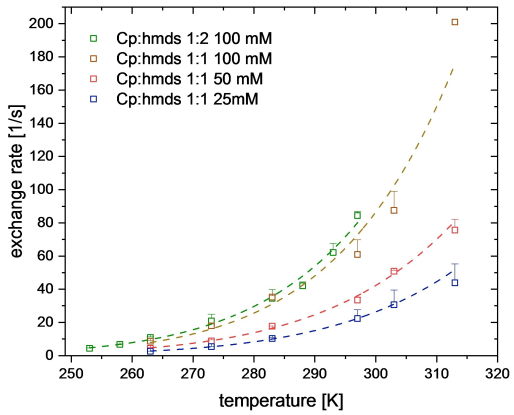

Figure 5. Influence of the concentration on the exchange rates of the equilibrium shown in Scheme 9 for the determination of the kinetic parameters $\Delta H^{\#}$ and $\Delta S^{\#}$ (see text).

the number of molecules. Now, the $[CpCa]^+$ cations can add to $Ca(hmds)_2$ yielding the ion $[CpCa(\mu\text{-}hmds)_2Ca(thf)_n]^+$ which could dissociate into heteroleptic CpCa(hmds) and $[Ca(hmds)]^+$. We propose that free hmds anions play a negligible role in this equilibrium whereas bridging hmds ligands are quite common in alkaline-earth metal chemistry as for example in ether-free $[(hmds)Ca(\mu\text{-}hmds)]_2$[47] and in $[(tmds)Ca(thf)(\mu\text{-}tmds)]_2$ (tmds = bis(dimethylsilyl)amide, $N(SiHMe_2)_2$).[48] For magnesocene dissociation processes have already been concluded based on electrochemical studies.[49] Therefore, similar dissociation reactions may be assumed for homologous calcium congeners because electrostatic attraction between cation and anion decreases significantly with increasing distance between contrary charges. To the best of our knowledge, bridging cyclopentadienide ligands are unknown in calcocene chemistry.

Taking into account that the calciate $[Ca(hmds)_3]^-$ (as free anion[50] and as counterion in contact ion pairs[51]) as well as ligated Cp'Ca(hmds)[52] and $[Ca(hmds)]^+$[53] have already been structurally authenticated, we propose the mechanism as

depicted in Scheme 11 for ligand scrambling and interconversion of homo- into heteroleptic compounds. In the calciate $[Ca(hmds)_3]^-$ the calcium atom is sterically shielded, and additional Lewis bases cannot be bonded. Therefore, heteroleptic anions such as $[CpCa(hmds)_2]^-$ with η^5-bound cyclopentadienide ligands are most likely too crowded and highly disadvantageous in this ligand redistribution system and hence neglected in Scheme 11. Based on these prerequisites the basic reactions are dissociation of $[(thf)_2CaCp_2]$ into $[CpCa]^+$ cations and Cp^- anions as well as aggregation of $[(thf)_2Ca(hmds)_2]$ (yielding $[(hmds)Ca(\mu\text{-}hmds)]_2$ under liberation of ligated thf) with subsequent dissociation into $[(thf)_nCa(hmds)]^+$ cations and $[Ca(hmds)_3]^-$ anions. Recombination of Cp^- anions and $[(thf)_nCa(hmds)]^+$ directly yields the heteroleptic product drawn with blue color. The $[CpCa]^+$ cation can add onto electroneutral $Ca(hmds)_2$ (under liberation of ligated thf) or onto $[Ca(hmds)_3]^-$ anions followed by dissociation along the dotted lines also leading to formation of $[(thf)_2Ca(hmds)Cp]$ shown in blue. The large entropy value for the transition state is caused by enhancement of the number of molecules via dissociation processes and liberation of thf bases.

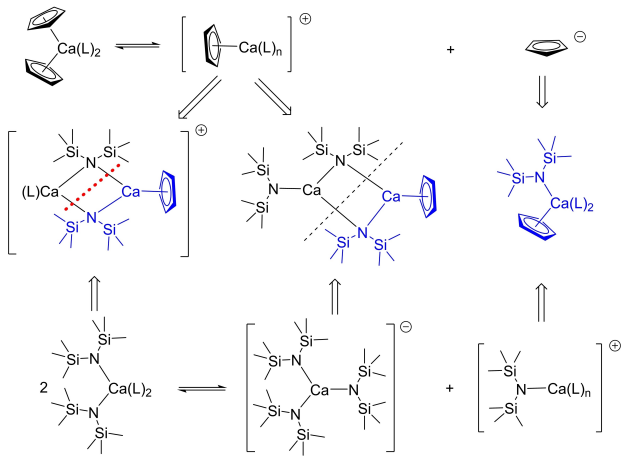

Scheme 11. Proposed mechanism for the ligand exchange between homoleptic calcocene and $Ca(hmds)_2$ on the one side and heteroleptic CpCa(hmds) on the other.

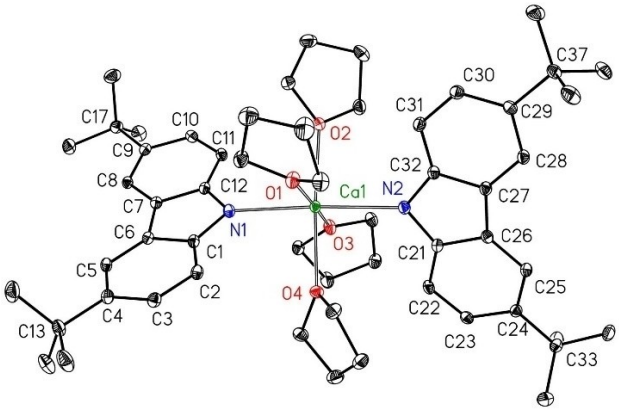

Figure 6. Molecular structure and atom labelling scheme of bis[3,6-di(tert-butyl)-9-carbazolyl]calcium $[(thf)_4Ca(Carb^{tBu2})_2]$. The ellipsoids represent a probability of 30%, H atoms are omitted for clarity reasons. Selected bond lengths (pm): Ca1–N1 242.93(18), Ca1–N2 244.86(19), Ca1–O1 237.31(16), Ca1–O2 236.95(17), Ca1–O3 237.72(16), Ca1–O4 237.67(16); angles (deg.): N1–Ca1–N2 176.73(7), N1–Ca1–O1 88.86(6), N1–Ca1–O2 91.89(6), N1–Ca1–O3 87.24(6), N1–Ca1–O4 91.90(6), N2–Ca1–O1 92.29(6), N2–Ca1–O2 91.20(6), N2–Ca1–O3 91.75(6), N2–Ca1–O4 85.01(6), O1–Ca1–O2 88.86(6), O1–Ca1–O3 175.26(6), O1–Ca1–O4 91.20(6), O2–Ca1–O3 88.58(6), O2–Ca1–O4 176.21(6), O3–Ca1–O4 91.62(6), Ca1–N1–C1 125.14(14), Ca1–N1–C12 131.02(14), Ca1–N2–C21 127.20(14), Ca1–N2–C32 128.50(14).

Molecular structures of selected complexes

The molecular structure and atom labelling scheme of the tetrakis(thf) adduct of bis[3,6-di(tert-butyl)-9-carbazolyl]calcium $[(thf)_4Ca(Carb^{tBu2})_2]$ are depicted in Figure 6. The calcium atom Ca1 is in a slightly distorted octahedral environment with the amides in trans position (N1–Ca1–N2 176.73(7)°) and oriented perpendicular to each other with the ligated thf molecules in the interspaces formed by these planar fluorenyl ligands. The proximal and distal Ca1–N1–C bond angles deviate only by a few degrees and verify negligible intramolecular steric strain. The molecular structure of the analogous indolyl complex $[(thf)_4Ca(Ind)_2]$ is shown in the Supporting Information (Figure S38) and has very similar structural parameters but the larger asymmetry of the indolyl ligands enhances slightly the difference between the proximal and distal Ca–N–C bond angles. The Ca–O distances vary in a narrow range between 236.95(17) and 237.72(16) pm verifying lack of steric pressure. The Ca1–N1 and Ca1–N2 bonds (242.93(18) and 244.86(19) pm, respectively) are slightly lengthened because the negative charge on the N-atom is reduced due to polarization of the aromatic π-system.

Bulkier amides stabilize smaller coordination numbers at calcium. Thus, the primary amide $[(thf)_3Ca\{NH\text{-}C_6H_2\text{-}2,4,6\text{-}(CHPh_2)_3\}_2]$ crystallizes as tri(thf) complex with crystallographic C_2 symmetry. Its molecular structure and atom labelling scheme are depicted in Figure 7. The calcium atom is in a trigonal bipyramidal environment with two thf ligands in apical positions. The bulky amide ligands are in the equatorial plane with a N1–Ca1–N1 A bond angle of 99.34(9)°. The Ca1–O1 and Ca1–O2 distances of 240.04(16) and 242.0(2) pm lie in a typical range whereas the Ca1–N1 bond length of 230.02(17) is rather small due to electrostatic attraction and smaller than observed in $[(thf)_4Ca(Fl^{tBu2})_2]$. The N1 atom is nearly trigonal planarly coordinated (angle sum 356°) allowing charge delocalization into the aryl substituent (N1–C1 136.9(2) pm). Comparable bonding parameters have been observed for other demanding primary amides of calcium.[54]

Calcocenes are a valuable substance class and the cyclopentadienide ligands can act as pseudohalides.[30] In addition, ligated ether bases can easily be exchanged via dissolution of the thf adducts of the calcocenes in appropriate ethereal solvents. As representative examples, the molecular structures and atom labelling schemes of bis(thf)-1,1′-bis(triisopropylsilyl)calcocene $[(thf)_2Ca(\eta^5\text{-}C_5H_4\text{-}TIPS)_2]$ and the diglyme adduct of decamethylcalcocene $[(diglyme)CaCp^*_2]$ are

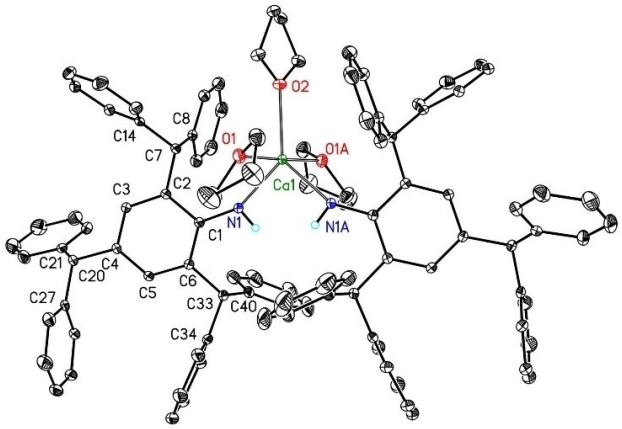

Figure 7. Molecular structure and atom labelling scheme of $[(thf)_3Ca\{NH\text{-}C_6H_2\text{-}2,4,6\text{-}(CHPh_2)_3\}_2]$. Ellipsoids represent a probability of 30%, C-bound hydrogen atoms are neglected for clarity reasons. Symmetry-related atoms (−x+1, y, −z+0.5) are marked with the letter "A". Selected bond lengths (pm): Ca1–N1 230.02(17), Ca1–O1 240.04(16), Ca1–O2 242.0(2), N1–C1 136.9(2), N1–$H1_{N1}$ 86(3); angles (deg.): N1–Ca1–N1 A 99.34(9), N1–Ca1–O1 89.39(6), N1–Ca1–O2 130.33(5), N1–O1 A 91.64(6), O1–Ca1–O2 89.20(4), O1–Ca1–O1 A 178.41(8), Ca1–N1–C1 147.16(15), Ca1–N1–$H1_{N1}$ 98.3(17), C1–N1–$H1_{N1}$ 110.4(17).

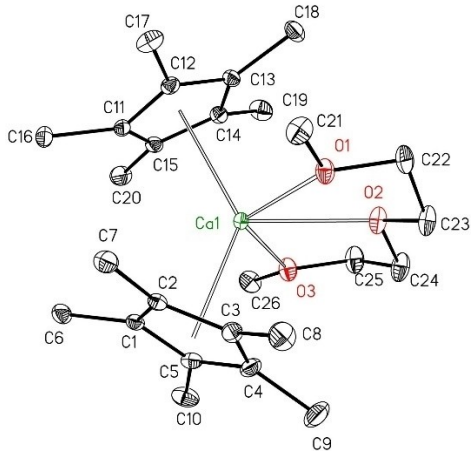

Figure 9. Molecular structure and atom labelling scheme of [(diglyme)CaCp*$_2$]. The ellipsoids represent a probability of 30%, hydrogen atoms are omitted. Selected bond lengths (pm): Ca1–O1 238.76(10), Ca1–C1 263.64(14), Ca1–C2 265.28(14), Ca1–C3 265.04(13), Ca1–C4 265.83(13), Ca1–C5 264.76(13), Ca1–C11 264.06(14), Ca1–C12 265.57(14), Ca1–C13 267.10(14), Ca1–C14 268.39(13), Ca1–C15 265.21(13).

depicted in Figures 8 and 9, respectively. As discussed above, Ca1–O1 and Ca1–O2 distances of 241.78(10) and 242.24(10) pm verify negligible intramolecular strain. The Ca1–C distances vary between 268.35(15) and 277.42(14) pm with the larger values to the carbon atoms carrying the bulky silyl substituents.

Despite the permethylation of the cyclopentadienide ligands in [(diglyme)CaCp*$_2$], diglyme binds via all oxygen donors to the calcium center. This binding mode leads to rather large Ca1–O1, Ca1–O2 and Ca1–O3 distances of 255.01(9), 262.73(9) and 261.43(9) pm. The induced steric pressure also elongates the Ca1–C bond lengths which vary between 274.67(12) and 289.20(12) pm being significantly larger than discussed above for $[(thf)_2Ca(\eta^5\text{-}C_5H_4\text{-}TIPS)_2]$. Expectedly, the bonding parameters of [(thf)CaCp*$_2$] (see Figure S40) are significantly smaller: Ca1–O1 238.76(10), Ca1–C between 263.64(14) and 268.39(13) pm and Δ(Ca–C) = 4.8 pm.

Additional ether adducts of decamethylcalcocene are presented in the Supporting Information. Selected structural data are summarized in Table 3. The mono(thf) adduct [(thf)CaCp*$_2$] has the lowest intramolecular strain and consequently, the smallest distances and the smallest tilt of the cyclopentadienide ligands and hence the smallest difference between smallest and largest Ca–C distances Δ(Ca–C). 1,2-Dimethoxyethane has a small bite and induces moderate steric pressure whereas another donor site in diglyme further enhances intramolecular strain.

Contrary to the significant changes of the structural parameters, exchange of ethereal ligands only induces very slight changes for the NMR parameters (Table 4). Substitution of

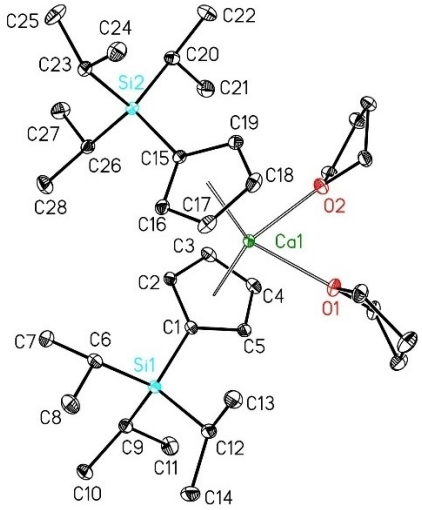

Figure 8. Molecular structure and atom labelling scheme of bis(thf)-1,1′-bis(triisopropylsilyl)calcocene $[(thf)_2Ca(\eta^5\text{-}C_5H_4\text{-}TIPS)_2]$. The ellipsoids represent a probability of 30%, H atoms are omitted for the sake of clarity. Selected bond lengths (pm): Ca1–O1 241.78(10), Ca1–O2 242.24(10), Ca1–C1 277.42(14), Ca1–C2 270.26(14), Ca1–C3 265.69(15), Ca1–C4 268.35(15), Ca1–C5 274.21(14), Ca1–C15 273.99(14), Ca1–C16 272.47(14), Ca1–C17 270.90(15), Ca1–C18 270.12(15), Ca1–C19 271.20(14); angle (deg.): O1–Ca1–O2 77.00(4).

Table 3. Selected structural parameters (bond lengths [pm], average values without standard deviations) of ether adducts of decamethylcalcocene CaCp*$_2$ and $[(thf)_2Ca(\eta^5\text{-}C_5H_4\text{-}TIPS)_2]$.

Compound	Ca–O	Ca–C_{min}	Ca–C_{max}	Δ(Ca–C)[a]
[(thf)CaCp*$_2$]	238.76(10)	263.64(14)	268.39(13)	4.8
$[(thp)_2CaCp^*_2]$	249.8	272.6(3)	277.7(3)	5.1
[(dme)CaCp*$_2$]	241.1	268.6(5)	273.3(5)	4.7
[(diglyme)CaCp*$_2$]	259.7	274.67(12)	289.20(12)	14.5
$[(thf)_2Ca(\eta^5\text{-}C_5H_4\text{-}TIPS)_2]$	242.01	265.69(15)	277.42(14)	11.7

[a] Difference between smallest and largest Ca–C bond length.

Table 4. NMR spectroscopic data (chemical shifts [ppm]) of ether adducts of decamethylcalcocene $CaCp^*_2$.[a]

Compound	$\delta(^1H)_{Me}$	$\delta(^{13}C)_{Me}$	$\delta(^{13}C)_{qC}$	$\Delta\delta(^{13}C)_{qC}$[b]
[(thf)$CaCp^*_2$]	2.01	10.6	112.0	0.0
[$(thf)_2CaCp^*_2$]	2.01	10.6	112.0	0.0
[$(Et_2O)CaCp^*_2$]	2.01	11.0	112.4	+0.4
[$(thp)_2CaCp^*_2$]	2.04	10.8	112.2	+0.2
[(dme)$CaCp^*_2$]	2.05	11.3	111.1	−0.9
[(diglyme)$CaCp^*_2$]	2.08	11.5	111.2	−0.8

[a] Solvent: [D_8]toluene, room temperature, 400 MHz. [b] Difference of the chemical shifts of the ring carbon atoms of the Cp* ligand, taking the thf complexes as reference.

thf by weaker monodentate or oligodentate ethers leads to a small low-field shift of the methyl resonances in ^1H and ^{13}C NMR spectra. For the ^{13}C NMR chemical shifts of the C_5-ring atoms a slight high-field shift is observed for complexes with the oligodentate bases dme and diglyme.

Formamidines, guanidines and β-diketimines show no reactivity under common reaction conditions of the *i*GMM. Nevertheless, these unsaturated amines can easily be deprotonated by stoichiometric amounts of $Ca(hmds)_2$. The molecular structure and atom labelling scheme of [$(thf)_3Ca\{HC(N\text{-}C_6H_3\text{-}2,6\text{-}F_2)_2\}_2$] are depicted in Figure 10. The calcium atom has the quite unusual coordination number 7. Nevertheless, the Ca1–O_{thf} bond lengths verify lack of significant intramolecular pressure. The N–C bond lengths within the 1,3-diazaallyl fragments are very similar due to complete charge delocalization. This finding is supported by very similar Ca1–N distances.

Compound [$(thf)_3Ca\{HC(N\text{-}C_6H_3\text{-}3,5\text{-}(CF_3)_2\}_2$] crystallizes with a very similar molecular structure that is depicted in Figure 11.

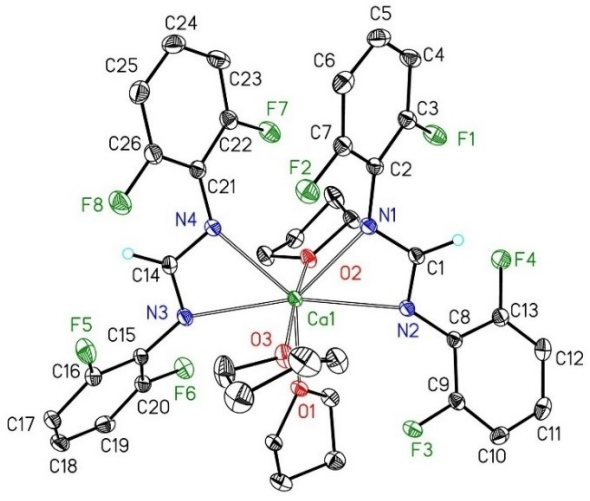

Figure 10. Molecular structure and atom labelling scheme of [$(thf)_3Ca\{HC(N\text{-}C_6H_3\text{-}2,6\text{-}F_2)_2\}_2$]. The ellipsoids represent a probability of 30%, H atoms are omitted except those at C1 and C14. Selected bond lengths (pm): Ca1–N1 249.35(16), Ca1–N2 252.65(16), Ca1–N3 255.69(16), Ca1–N4 246.49(17), Ca1–O1 240.16(14), Ca1–O2 236.41(14), Ca1–O3 238.01(14), N1–C1 131.2(3), N2–C1 132.4(2), N3–C14 131.3(3), N4–C14 132.1(3); angles (deg.): C1–N1–C2 119.82(17), N1–C1–N2 117.55(17), C1–N2–C8 119.70(16), C14–N3–C15 118.73(17), N3–C14–N4 118.36(18), C14–N4–C21 119.47(17).

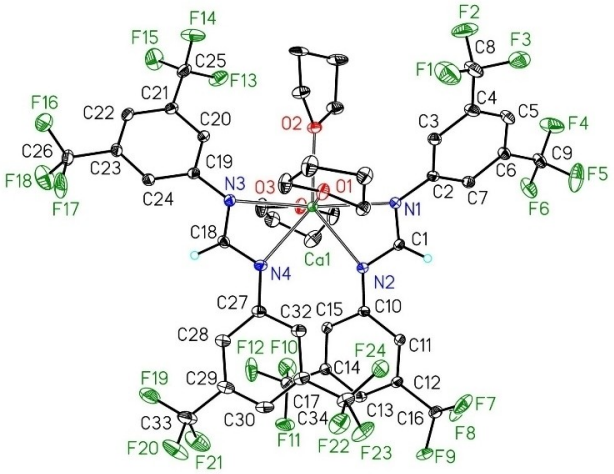

Figure 11. Molecular structure and atom labelling scheme of [$(thf)_3Ca\{HC(N\text{-}C_6H_3\text{-}3,5\text{-}(CF_3)_2\}_2$]. The ellipsoids represent a probability of 30%, H atoms are neglected except those at C1 and C18. Selected bond lengths (pm): Ca1–N1 250.7(2), Ca1–N2 248.4(2), Ca1–N3 249.8(2), Ca1–N4 246.9(2), Ca1–O1 240.3(2), Ca1–O2 239.9(2), Ca1–O3 243.2(2), N1–C1 132.4(3), N2–C1 132.3(3), N3–C18 132.1(4), N4–C18 132.5(4); angles (deg.): C1–N1–C2 119.3(2), N1–C1–N2 117.4(2), C1–N2–C10 121.1(2), C18–N3–C19 121.3(2), N3–C18–N4 117.0(3), C18–N4–C27 122.2(2).

The fact that the trifluoromethyl groups are bound in 3,5-positions reduces intramolecular strain leading to slightly smaller Ca1–N bond lengths. The calcium atom has a slightly distorted pentagonal bipyramidal coordination sphere with the oxygen atoms O1 and O3 in apical positions (O1–Ca1–O3 169.26(8)°).

Larger substituents in ortho-position of the *N*-bound aryl substituents reduce the coordination number of the alkaline-earth metal, and [$(thf)_2Ca\{HC(N\text{-}C_6H_3\text{-}2,6\text{-}i\text{Pr}_2)_2\}_2$] contains a six-coordinate calcium atom. Molecular structure and atom labelling scheme of this complex are depicted in Figure 12. The coordination sphere of calcium is best described as a distorted trigonal prism with the trigonal faces built by O1/N1/N2A and N2/O1A/N1A. The smaller coordination number leads to smaller Ca1–N bond lengths whereas the Ca–O_{thf} distances lie in the same range as discussed above due to steric hindrance between the ether ligands and the ortho-isopropyl groups. Therefore, it is not astonishing that also the mono(thf) adduct [$(thf)Ca\{HC(N\text{-}C_6H_3\text{-}2,6\text{-}i\text{Pr}_2)_2\}_2$] has already been described.[55] Enhancement of steric hindrance by an additional alkyl substituent at the carbon atom of the 1,3-diazaallyl fragment even allows stabilization of [$Ca\{t\text{BuC}(N\text{-}C_6H_3\text{-}2,6\text{-}i\text{Pr}_2)_2\}_2$] with a four-coordinate calcium center and without additional ligated ether bases.[56] In contrast, smaller aryl groups allow coordination of an additional diethyl ether molecule as observed in [$(Et_2O)Ca\{t\text{BuC}(N\text{-}C_6H_2\text{-}2,4,6\text{-}Me_3)_2\}_2$].[57] Compounds with less bulky *N*-bound aryl groups crystallize with two ligated thf bases as observed earlier for [$(thf)_2Ca\{HC(N\text{-}C_6H_3\text{-}2,6\text{-}Me_2)_2\}_2$] and [$(thf)_2Ca\{HC(N\text{-}C_6H_4\text{-}2\text{-}Me)_2\}_2$].[58]

The synthesis and isolation of calcium amidinates verified that $Ca(hmds)_2$ quantitatively converted bulky amidines into their calcium amidinates and hence, the pK_a values of the

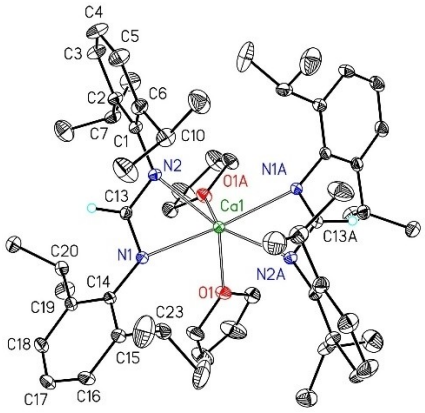

Figure 12. Molecular structure and atom labelling scheme of $[(thf)_2Ca\{HC(N\text{-}C_6H_3\text{-}2,6\text{-}iPr_2)_2\}_2]$. The ellipsoids represent a probability of 30%, H atoms are neglected for clarity reasons except those at C13. Symmetry-equivalent atoms (−x+1, y, −z+1.5) are marked with the letter "A". Selected bond lengths (pm): Ca1–N1 247.26(17), Ca1–N2 242.28(16), Ca1–O1 242.42(15), N1–C13 131.9(2), N2–C13 132.6(2); angles (deg.): C13–N1–C14 118.60(18), N1–C13–N2 120.77(18), C1–N2–C13 117.54(17).

amidines lie in a suitable region. Therefore, the catalytic conversion via the *i*GMM had been included in our investigations. Thus, bromoethane was added at room temperature to a suspension of calcium and amidine in THF in the presence of 10 mol-% of H(hmds). However, we isolated the appropriate amount of 10 mol-% of calcium-bound amidinates but H(hmds) was unable to promote a catalytic conversion.

This finding can be explained by different competing reactions with significantly different reaction rates. The first step is formation of EtCaBr which can then react either with H(hmds) (yielding $Ca(hmds)_2$) or with amidine (giving calcium amidinates) or with EtBr (forming the *Wurtz*-type coupling product butane). In *N,N'*-diarylamidines the acidic N–H functionality is sterically shielded disfavoring the deprotonation reaction and therefore, the *Wurtz*-type coupling reaction prevails over the metalation of the amidines. The slow reaction of $Ca(hmds)_2$ with amidines finally leads to the formation of amidinates and H(hmds), but due to the fact that all EtBr has already been consumed, the reaction ceases and the amidine remains unchanged.

Conclusions

The in situ *Grignard* metalation method (*i*GMM) represents a powerful tool to quickly synthesize *Hauser* bases R_2N-MgBr with high yields and in multi-gram scale in ethereal solvents. These reagents can show *Schlenk*-type dismutation reactions yielding homoleptic $Mg(NR_2)_2$ and $MgBr_2$. Transfer of the *i*GMM to the homologous calcium chemistry exhibits advantages but also some limitations and restrictions. In a typical protocol, bromoethane is added to a suspension of calcium and H-acidic substrate in an ethereal solvent, preferably THF. In hydrocarbon solvents, no reaction occurs. Activation of calcium prior to use is unnecessary for a smooth and straightforward conversion. Contrary to the magnesium-based procedure, homoleptic calcium compounds such as calcium bis(amides) are isolated even though that initially formed EtCaBr shows a *Schlenk*-type equilibrium. This strategy allows high-yield and straightforward synthesis of $Ca(hmds)_2$ in THF whereas bulkier substrates lead to significantly lower yields or show no conversion at all, regardless of their pK_a values. This finding underlines the tremendous steric influence of bulky groups on the suitability of this procedure. An important aspect is solubility in THF, otherwise precipitate covers the calcium granules and the reaction ceases. In addition, side reactions compete with the formation of the calcium reagents. The major side products arise from ether degradation processes (especially above room temperature) and from *Wurtz*-type coupling reactions (especially at low temperatures below 0 °C).

Pure $Ca(hmds)_2$ is easily accessible with large amounts within a few hours providing a powerful calcium-based reagent for stoichiometric conversions. Thus, shielded *N,N'*-diarylamidines cannot be calciated via the *i*GMM but a stoichiometric metalation with $Ca(hmds)_2$ works nicely. This observation suggests the addition of catalytic amounts of H(hmds) to the ethereal suspension of calcium and *N,N'*-diarylamidine but this dodge fails because shielding of the H-acidic functionality decelerates the metalation reactions which is in favor of the *Wurtz*-type coupling side reaction and hence primary formation of butane.

In summary, we established a very beneficial protocol for a straightforward one-pot synthesis of $Ca(hmds)_2$ in THF without the necessity of metal activation prior to use. The *i*GMM can be transferred to many unshielded H-acidic substrates whereas for sterically shielded H-acidic compounds stoichiometric procedures of $Ca(hmds)_2$ with the substrate are recommended. Bulky groups strongly decelerate deprotonation processes and *Wurtz*-type coupling becomes the dominant reaction.

Experimental Section

General information: All manipulations were carried out under an inert nitrogen atmosphere using standard *Schlenk* techniques, if not otherwise noted. The solvents were dried over KOH and subsequently distilled over sodium/benzophenone under a nitrogen atmosphere prior to use. All substrates were purchased from Alfa Aesar, abcr, Sigma Aldrich or TCI and used without further purification. 3,6-Di(tert-butyl)carbazole was synthesized as described in the literature.[59] The yields given are not optimized. Purity of the compounds was verified by NMR spectroscopy. Deuterated solvents were dried over sodium, distilled, degassed, and stored under nitrogen over sodium. ^1H, and $^{13}C\{^1H\}$ NMR spectra were recorded on Bruker Avance I 250 (BBO) Bruker Avance III 400 (BBO, BBFO probes Avance neo 500 (BBFO Prodigy probe) and Avance III HD 600 (TCI cryoprobe) spectrometers. Chemical shifts are reported in parts per million relatively to $SiMe_4$ as an external standard referenced to the solvents residual proton signal using xiref AU program for ^{13}C NMR spectra. DOSY NMR spectra were measured using the convection compensated dstebpgp3 s standard pulse sequence. Molar masses in solution were calculated using the *Stalke*-ECC-DOSY method (standard: adamantane or $Si(SiMe_3)_4$).[60] ASAP-HSQC spectra and ASAP-HSQC-DEPT spectra were recorded using the published pulse sequences.[61] All HPLC

runs were performed using an Ultimate 3000 UPLC with a Chromasil C-18 column and MeOH/H_2O as eluent. Quantitative measurements based on peak areas in the chromatogram. Elemental analyses of the calcium compounds gave no reproducible and reliable results due to loss of ligated ether bases and formation of carbonates and carbides during handling and combustion.

General procedure for synthesis of fluorine containing amidinates (according to a published procedure):[62] Fluoroaniline (100 mmol, 2 equiv.) and triethylorthoformiate (50 mmol, 1 equiv.) were placed in a round bottom flask and HCl (aqueous, 35%, 1 drop) was added under stirring. After stirring for 30 min at room temperature the formed solid was separated and washed with *n*-pentane (3×20 mL). The solid was dried under reduced pressure and the fluorine-containing amidinates were isolated as colorless, crystalline solids.

General procedure for synthesis of alkyl calcium compounds (Table 1): Calcium or activated calcium powder (1.2 equiv., 1 g, 2.5 mmol) were placed in a *Schlenk* flask and THF (20 mL) was added. Alkyl halide (1/20 equiv.) was added, and the mixture was stirred for five minutes at room temperature. The reaction mixture was cooled to the desired temperature and alkyl halide (1 equiv.) in THF (20 mL) was added slowly over 30 min. After the reaction time of 2–15 h the suspension was filtered over a precooled G3 frit with diatomaceous earth. An aliquot of the filtrate was hydrolyzed and titrated with sulphuric acid against phenolphthalein. NMR samples were prepared by removal of the solvent under reduced pressure of an aliquot, dissolution of the residue in [D_8]THF and immediate measurement of ^{1}H NMR spectra. NMR data of $(thf)_nCaMe_2$ were already published by *Anwander* and coworkers.[39] $(thf)_nCa(Et)_2$: ^{1}H NMR (400 MHz, [D_8]THF, 297 K): 1.34 (t, 3H J=8.2 Hz, CH_2CH_3), −0,90 (q, 2H J=8.2 Hz, CH_2CH_3). $(thf)_nCa(Et)(Br)$: ^{1}H NMR (400 MHz, [D_8]THF, 297 K): 1.32 (br, 3H, CH_2CH_3), −0,73 (br, 2H, CH_2CH_3).

***N,N′*-Bis(2,6-difluorophenyl)formamidine**: Applied quantity: 96 mmol of 2,6-difluoroaniline, yield: 10,1 g, 79%; ^{1}H NMR (300 MHz, $CDCl_3$, 297 K): δ=8.41 (s, 1H), 6.86 (m, 6H) ppm; ^{13}C NMR (75 MHz, $CDCl_3$, 297 K): δ=156.8 (d, J=5.7 Hz), 153.5 (d, J=5.8 Hz), 123.2 (t, J=9.8 Hz), 112.3–111.5 (m) ppm. ^{19}F NMR (376.5 MHz, $CDCl_3$, 297 K): δ=−125.0 ppm.

***N,N′*-Bis(2-fluorophenyl)formamidine**: Applied quantity: 60 mmol of 2-fluoroaniline, yield: 4,8 g, 21 mmol, 67%, ^{1}H NMR (300 MHz, $CDCl_3$, 297 K): δ=8.26 (s, 1H), 7.33 (s, 2H), 7.21–6.93 (m, 6H) ppm. ^{13}C NMR (75 MHz, $CDCl_3$, 297 K): δ=153.9 (d, J=245.0 Hz), 124.7 (d, J=3.8 Hz), 124.0 (d, J=7.5 Hz), 115.9 (d, J=19.7 Hz) ppm. ^{19}F NMR (376.5 MHz, $CDCl_3$, 297 K): δ=−130.0 ppm.

***N,N′*-Bis[3,5-bis(trifluoromethyl)phenyl]formamidine**: Applied quantity: 60 mmol of 3,5-bis(trifluoromethyl)aniline, yield: 7,5 g, 16 mmol, 53%, ^{1}H NMR (400 MHz, $CDCl_3$, 297 K): δ=8.14 (s, 1H), 7.63 (m, 6H) ^{13}C NMR (101 MHz,[D_6]Acetone, 297 K): δ=198.4, 180.3 (q, J=33.0 Hz), 175.9, 171.9 (d, J=271.9 Hz), 164.2 ppm ^{19}F NMR (376.5 MHz, $CDCl_3$, 297 K): δ=−62.5 ppm.

Tris(tetrahydrofuran)calcium-bis[*N,N′*-bis(2,6-difluorophenyl)-formamidinate]: *N,N′*-Bis(2,6-difluorophenyl)formamidine (1,0 g, 3,7 mmol, 2 equiv.) was dissolved in THF (5 mL) and $Ca(hmds)_2$ (0,5 M in THF, 3,7 mL, 1,8 mmol, 1 equiv.) was added and the reaction mixture stirred for 30 min. Then it was stored for 24 h at −20 °C. During this time colorless crystals precipitated which were suitable for single crystal diffraction experiments. Yield: 1.2 g, 1.6 mmol, 86%. ^{1}H NMR (400 MHz, 297 K, [D_8]THF): δ=6,27 (br, 1H CH), 4,91 (br, 6H, CH_{arom}) ppm. ^{13}C NMR (101 MHz, 297 K, [D_8]THF): δ=168,45, 158,36, 155,97, 130,27, 118,86 ppm. ^{19}F NMR (376 MHz, 297 K, [D_8]THF): δ=−126,7 ppm.

Tris(tetrahydrofuran)calcium-bis[*N,N′*-bis{3,5-bis(trifluoromethyl)phenyl}-formamidinate]: $(thf)_2Ca(hmds)_2$ (90.5 mg, 179 μmol, 1 equiv.) was dissolved in THF (1 mL) and *N,N′*-bis[3,5-bis(trifluoromethyl)phenyl]formamidine (160 mg, 351 μmol, 2 equiv.) was added in one portion. The clear, slightly yellow solution was evaporated to dryness and the residue was dissolved in [D_8]THF. The proton NMR spectrum verified full conversation to the calcium bis(formamidinate). Suitable crystals for single crystal diffraction measurements were grown from a saturated THF solution at −20 °C. Yield: 35 mg, 33 μmol, 19%. ^{1}H NMR (400 MHz, 297 K, [D_8]Tol): δ=8.66 (s, 1H), 7.50 (s, 2H), 7.25 (s, 4H), 3.48 (br, 8H), 1.37 (br, 8H) ppm. ^{13}C NMR (101 MHz, 297 K, [D_8]Tol): δ=162.4, 152.4, 132.5 (q, J=32.6 Hz), 122.5, 119.1 (d, J=4.0 Hz), 114.1, 68.5 (thf), 24.9 (thf) ppm. ^{19}F NMR (376.5 MHz, 297 K, [D_8]toluene): δ=−62,9 ppm, IR (ATR, cm^{-1}): 2956 (w), 2887 (w), 1537 (m), 1523 (m), 1362 (s), 1089 (s).

Bis(tetrahydrofuran)calcium-bis[*N,N′*-bis(2,6-di*iso*propylphenyl)-formamidinate]: *N,N′*-Bis(2,6-di*iso*propylphenyl)formamidine (600 mg, 1.65 mmol, 2 equiv.) was placed in a *Schlenk* tube and $Ca(hmds)_2$ (0.19 M in *n*-Pentan, 0.82 mmol, 4,33 mL) was added. The reaction mixture was stirred for 30 min at room temperature. To the slightly turbid solution THF was added under heating to 30 °C until a clear solution formed. After cooling to room temperature and storage for 48 h, the calcium bis(formamidinate) crystallized in the shape of big colorless cubes (yield: 452 mg, 0.496 mmol, 61%). ^{1}H NMR (400 MHz, 297 K, [D_8]THF): δ=7.63 (s, 1H), 6.88 (d, J=7.6 Hz, 4H), 6.76 (dd, J=8.2, 7.0 Hz, 2H), 3.33 (p, J=6.8 Hz, 4H), 0.94 (d, J=6.9 Hz, 24H) ppm. ^{13}C NMR (101 MHz, 297 K, [D_8]THF): δ=169.1, 148.9, 143.3, 123.0, 122.7, 27.8 ppm, IR (ATR, cm^{-1}): 3081 (w), 3024 (m), 2960 (m), 2924 (m), 2863 (w), 1663 (m), 1519 (m), 1451 (s).

Bis[3,6-di(tert-butyl)-9-carbazolyl]calcium: $[(thf)_2Ca(hmds)_2]$ (0.5 M in THF, 1 mL, 0.5 mmol, 1 equiv.) was added dropwise to a solution of 3,6-di(tert-butyl)-9-carbazole (280 mg, 1 mmol, 2 equiv.) in THF (5 mL). After 5 minutes a few small crystals precipitated from the solution. The solution was heated to 50 °C and slowly cooled to room temperature. During 24 h at room temperature, colorless crystals precipitated which were collected and dried in vacuo (yield: 248 mg, 0.3 mmol, 56%). ^{1}H NMR (400 MHz, [D_8]THF, 297 K): δ=8.03 (d, J=2.0 Hz, 2H), 7.39–7.12 (m, 4H), 3.60 (m, thf), 1.76 (m, thf), 1.42 (s, 18H) ppm. ^{13}C{^{1}H} NMR (101 MHz, C_6D_6, 297 K): δ=150.2, 135.4, 125.1, 119.6, 114.6, 113.2, 34.0, 31.9 ppm.

$[(thf)_3Ca\{HN\text{-}C_6H_2\text{-}2,4,6\text{-}(CHPh_2)_3\}_2]$: $[(thf)_2Ca(hmds)_2]$ (0.175 g, 0.346 mmol, 1 equiv.) and 2,4,6-tris(diphenylmethyl)aniline (0.410 g, 0.692 mmol, 2 equiv.) were dissolved in THF (15 mL). After 3 min a clear slightly yellow solution formed. At room temperature a colorless solid precipitated within 30 minutes. Recrystallization from hot THF yielded colorless crystals of the anilide (410 mg, 0,285 mmol, 82%). ^{1}H NMR (600 MHz, [D_8]toluene, 297 K): δ=6.89 (m, 36 H), 6.56 (s, 2H, CHAryl), 5.30 (s, 2H, CH), 5.0 (s, 1H, para-CH), 3.10 (br, 1H, NH) ppm.

$[(thf)_2CaCp_2]$: Calcium granules (4,5 g, 112 mmol, 1 equiv.) and freshly distilled CpH (9,3 mL, 112 mmol, 1 equiv.) were suspended in THF (107 mL). EtBr (8,4 mL, 112 mmol, 1 equiv.) was added in one portion at room temperature. After five minutes gas evolution and formation of a precipitate started. After 17–20 h no further gas evolution ceased, and the suspension was allowed to settle. Titration of a hydrolyzed aliquot of the supernatant solution with H_2SO_4 against phenolphthalein showed an alkalinity of 0,71 M (71%). The suspension was filtered (G3 with diatomaceous earth) and the clear filtrate was stored at −40 °C for 24 h. During this time $(thf)_2Ca(Cp)_2$ crystalized in the shape of large colorless cubes. The precipitate was collected on a G1 frit and dried in vacuo (4.4 g, 14 mmol, 25%). The mother liquor could be used directly as solvent for the preparation of a new batch. ^{1}H NMR (400 MHz, [D]$_8$toluene,

297 K): δ = 6.12 (br, 10H), 3.40 (br, 8H, THF), 1.34 (br, 8H, THF) ppm. ^{1}H DOSY NMR (400 MHz, [D]$_8$toluene, 297 K): D(adamantane) = 1.80×10^{-9} m^2/s, D = 1.19×10^{-9} m^2, MW = 295 g/mol, MW ([(thf)$_2$CaCp$_2$]) = 314, Δ = 6%. ^{1}H DOSY NMR (400 MHz, [D]$_8$THF, 297 K): D(adamantane) = 1.37×10^{-9} m^2/s, D = 0.87×10^{-9} m^2, MW = 334 g/mol, MW ([(thf)$_2$CaCp$_2$]) = 314, Δ = 1%. ^{13}C NMR (101 MHz, [D]$_8$toluene, 297 K) = 107.2, 67.9, 37.7 ppm.

[(thf)$_2$Ca(^{TIPS}Cp)$_2$]: ^{TIPS}CpH (2 g, 9 mmol, 1 equiv.) and calcium (350 mg, 9 mmol, 1 equiv.) were suspended in THF (35 mL). EtBr (700 μL, 9 mmol, 1 equiv.) was added in one portion. The reaction mixture was stirred overnight at room temperature. An aliquot (1 mL) was hydrolyzed and titrated with sulphuric acid against phenolphthalein (conversion: 53%). After addition of a second equivalent of EtBr (700 μL, 1 equiv.) and stirring overnight, the yield increased to 74%. The suspension was filtered (G3, diatomaceous earth) and washed with THF (5 mL). The volume of the filtrate was reduced to 1/5. *n*-Pentane (15 mL) was added, the supernatant solution was decanted and stored at −20 °C. After two weeks colorless crystals precipitated which were suitable for single crystal diffractometry. ^{1}H NMR (400 MHz, C_6D_6, 297 K): δ = 1.22–1.24 (m, 36H, TIPS), 1.29 (m, 8H, THF), 1.38 (m, 6H, TIPS), 3.42 (m, 8H, TIPS), 6.29 (t, *J* = 2.5 Hz, 4H, Cp), 6.52 (t, *J* = 2.5 Hz, 4H, Cp) ppm. ^{13}C NMR (101 MHz, C_6D_6, 297 K): δ = 12.4, 19.4, 25.0, 69.1, 110.9, 111.0, 118.6 ppm. ^{29}Si NMR (78.5 MHz, C_6D_6, 297 K): δ = −1.3 ppm, IR (ATR, cm^{-1}): 3078 (m), 2887 (w), 2860 (s), 1461 (m), 1060 (s), 881 (s), 815 (s), 662 (s).

CaCp*$_2$ adducts: CaCp*$_2$ (2 mmol) was placed in a *Young* tube, the appropriate donor solvent (1–2 equiv.) and C_6D_6 (0.55 mL) were added. The formed adducts were characterized by NMR spectroscopy and the structure in solution was verified by ECC-DOSY measurements.

Crystal Structure Determinations: The intensity data for the compounds were collected on a Nonius KappaCCD diffractometer using graphite-monochromated Mo-K$_\alpha$ radiation. Data were corrected for Lorentz and polarization effects; absorption was taken into account on a semi-empirical basis using multiple-scans.[63–66] The structures were solved by intrinsic methods (SHELXT)[67] and refined by full-matrix least squares techniques against F_o^2 SHELXL-2018).[68] The hydrogen atoms bonded to the formamidinato carbon atoms of [(thf)$_3$Ca{HC(N-C$_6$H$_3$-3,5-(CF$_3$)$_2$}$_2$], [(thf)$_3$Ca{HC(N-C$_6$H$_3$-2,6-F$_2$)$_2$}$_2$], [(thf)$_2$Ca{HC(N-C$_6$H$_3$-2,6-*i*Pr$_2$)$_2$}$_2$], and to the amide groups of [(thf)$_3$Ca{NH-C$_6$H$_2$-2,4,6-(CHPh$_2$)$_3$}$_2$] were located by difference Fourier synthesis and refined isotropically. All other hydrogen atoms were included at calculated positions with fixed thermal parameters. The crystals of [(thp)$_2$CaCp*$_2$] and [(thf)$_4$Ca(Ind)$_2$] were non-merohedral twins. The twin laws were determined to (−1.000 0.000 0.000) (0.000 −1.000 0.000) (0.165 0.000 1.000) and (−1.000 −0.025 0.026) (−0.009 −0.102 −0.901) (0.010 −1.098 0.102), respectively.[69] The contributions of the main components were refined to 0.787(4), and 0.620(2), respectively. The crystals of [(thf)$_3$Ca{HC(N-C$_6$H$_3$-3,5-(CF$_3$)$_2$}$_2$], [(thf)$_3$Ca{HC(N-C$_6$H$_3$-2,6-F$_2$)$_2$}$_2$] and [(thf)$_3$Ca{NH-C$_6$H$_2$-2,4,6-(CHPh$_2$)$_3$}$_2$] contain large voids, filled with disordered solvent molecules. The sizes of the voids are 429, 1250, and 739 Å^3/unit cell, respectively. Their contribution to the structure factors was secured by back-Fourier transformation using the SQUEEZE routine of the program PLATON[69] resulting in 82, 532, and 298 electrons/unit cell, respectively. Disordered moieties of [(dme)CaCp*$_2$], [(thf)$_4$Ca(Ind)$_2$], [(thf)$_3$Ca{HC(N-C$_6$H$_3$-3,5-(CF$_3$)$_2$}$_2$], [(thf)$_3$Ca{HC(N-C$_6$H$_3$-2,6-F$_2$)$_2$}$_2$], [(thf)$_2$Ca{HC(N-C$_6$H$_3$-2,6-*i*Pr$_2$)$_2$}$_2$], and [(thf)$_3$Ca{NH-C$_6$H$_2$-2,4,6-(CHPh$_2$)$_3$}$_2$] were refined using bond length restraints and displacement parameter restraints.[68] All non-hydrogen atoms were refined anisotropically.[68] Crystallographic data as well as structure solution and refinement details are summarized in Table S1. XP[70] was used for structure representations.

Deposition Number(s) 2172915 (for [(thf)$_2$CaCp$_2$]), 2172916 (for [(thf)CaCp*$_2$]), 2172917 (for [(dme)CaCp*$_2$]), 2172918 (for [(diglyme)CaCp*$_2$]), 2172919 (for [(thp)$_2$CaCp*$_2$]), 2172920 (for [(thf)$_4$Ca(Carb^{tBu2})$_2$]), 2172921 (for [(thf)$_2$Ca(η^5-C$_5$H$_4$-TIPS)$_2$]), 2172922 (for [(thf)$_4$Ca(Ind)$_2$]), 2172923 (for [(thf)$_3$Ca{HC(N-C$_6$H$_3$-3,5-(CF$_3$)$_2$}$_2$]), 2172924 (for [(thf)$_3$Ca{HC(N-C$_6$H$_3$-2,6-F$_2$)$_2$}$_2$]), 2172925 (for [(thf)$_2$Ca{HC(N-C$_6$H$_3$-2,6-*i*Pr$_2$)$_2$}$_2$]), and 2172926 (for [(thf)$_3$Ca{NH-C$_6$H$_2$-2,4,6-(CHPh$_2$)$_3$}$_2$]) contain(s) the supplementary crystallographic data for this paper. These data are provided free of charge by the joint Cambridge Crystallographic Data Centre and Fachinformationszentrum Karlsruhe Access Structures service.

Supporting Information

NMR spectra, crystallographic and structure refinement details, molecular representations of [(thf)$_4$Ca(Ind)$_2$], [(thf)$_2$CaCp$_2$], [(thf)CaCp*$_2$], [(dme)CaCp*$_2$], and [(thp)$_2$CaCp*$_2$] (pdf format).

Acknowledgements

We acknowledge the valuable support of the NMR service platform (www.nmr.uni-jena.de/) of the Faculty of Chemistry and Earth Sciences of the Friedrich Schiller University Jena, Germany. Parts of the equipment were provided by the German Research Foundation (DFG, INST 275/442-1 FUGG) which we kindly acknowledge. P. Schüler is very grateful to the German Environment Foundation (Deutsche Bundesstiftung Umwelt, DBU, grant no. 20018/578) for a generous Ph.D. grant. We thank L. Skodda and T. Schütt for support in the frame of their advanced chemistry laboratory courses. Open Access funding enabled and organized by Projekt DEAL.

Conflict of Interest

The authors declare no conflict of interest.

Data Availability Statement

The data that support the findings of this study are available in the supplementary material of this article.

Keywords: amides · calcium · calcocenes · in situ *Grignard* metalation method · metalation reactions

[1] Part I: S. Sengupta, P. Schüler, H. Görls, P. Liebing, S. Krieck, M. Westerhausen, *Chem. Eur. J.* **2022**, *28*, e202201359.
[2] A. F. Holleman, E. Wiberg, N. Wiberg, in *Inorganic Chemistry*, Academic Press, San Diego, **2001**.
[3] A. Koch, S. Krieck, H. Görls, M. Westerhausen, *Inorganics* **2016**, *4*, 39.
[4] a) W. J. Mc Creary, *J. Metals* **1958**, *10*, 615–617; b) J. Evers, A. Weiss, E. Kaldis, J. Muheim, *J. Less-Common Met.* **1973**, *30*, 83–95.
[5] a) M. A. Zemlyanichenko, N. I. Sheverdina, V. A. Chernoplekova, K. A. Kocheshkov, *Zh. Obshch. Khim.* **1972**, *42*, 841–843; b) I. E. Paleeva, N. I. Sheverdina, K. A. Kocheshkov, *Dokl. Akad. Nauk SSSR* **1973**, *210*, 1134–1135; c) I. E. Paleeva, N. I. Sheverdina, K. A. Kocheshkov, *Zh. Obshch. Khim.* **1974**, *44*, 1135–1137.

[6] a) R. D. Rieke, *Acc. Chem. Res.* **1977**, *10*, 301–306; b) R. D. Rieke, *Science* **1989**, *246*, 1260–1264; c) T.-C. Wu, H. Xiong, R. D. Rieke, *J. Org. Chem.* **1990**, *55*, 5045–5051; d) M. J. McCormick, K. B. Moon, S. R. Jones, T. P. Hanusa, *J. Chem. Soc. Chem. Commun.* **1990**, 778–779; e) R. D. Rieke, M. V. Hanson, *Tetrahedron* **1997**, *53*, 1925–1956. For a general overview on metal activation see: A. Fürstner, *Angew. Chem.* **1993**, *105*, 171–197; *Angew. Chem. Int. Ed.* **1993**, *32*, 164–189.

[7] H. Bönnemann, B. Bogdanovic, R. Brinkmann, N. Egeler, R. Benn, I. Topalovic, K. Seevogel, *Main Group Met. Chem.* **1990**, *13*, 341–362.

[8] a) K. J. Klabunde, *Acc. Chem. Res.* **1975**, *8*, 393–399; b) K. Mochida, S.-i. Ogura, T. Yamanishi, *Bull. Chem. Soc. Jpn.* **1986**, *59*, 2633–2634; c) K. Mochida, T. Yamanishi, *J. Organomet. Chem.* **1987**, *332*, 247–252.

[9] W. C. Johnson, M. F. Strubbs, A. E. Sidwell, A. Pechukas, *J. Am. Chem. Soc.* **1939**, *61*, 318–329.

[10] R. Fischer, M. Gärtner, H. Görls, M. Westerhausen, *Organometallics* **2006**, *25*, 3496–3500.

[11] a) M. Westerhausen, *Trends Organomet. Chem.* **1997**, *2*, 89–105; b) M. Westerhausen, *Coord. Chem. Rev.* **1998**, *176*, 157–210; c) A. Torvisco, A. Y. O'Brien, K. Ruhlandt-Senge, *Coord. Chem. Rev.* **2011**, *255*, 1268–1292; d) M. P. Coles, *Coord. Chem. Rev.* **2015**, *297–298*, 2–23.

[12] a) P. Jutzi, *Adv. Organomet. Chem.* **1986**, *26*, 217–295; b) P. Jutzi, *J. Organomet. Chem.* **1990**, *400*, 1–17; c) T. P. Hanusa, *Chem. Rev.* **1993**, *93*, 1023–1036; d) D. J. Burkey, T. P. Hanusa, *Comments Inorg. Chem.* **1995**, *17*, 41–77; e) A. J. Bridgeman, *J. Chem. Soc. Dalton Trans.* **1997**, 2887–2893; f) P. Jutzi, N. Burford in *Metallocenes: Synthesis, Reactivity, Applications, Vol. 1* (Eds.: A. Togni, R. L. Halterman), Wiley-VCH, Weinheim, **1998**, pp. 3–54; g) N. J. Long, in *Metallocenes: An Introduction to Sandwich Complexes*, Blackwell Science, Oxford, **1998**; h) P. Jutzi, N. Burford, *Chem. Rev.* **1999**, *99*, 969–990; i) P. Jutzi, G. Reumann, *J. Chem. Soc. Dalton Trans.* **2000**, 2237–2244; j) T. P. Hanusa, *Organometallics* **2002**, *21*, 2559–2571; k) P. H. M. Budzelaar, J. J. Engelberts, J. H. van Lenthe, *Organometallics* **2003**, *22*, 1562–1576.

[13] a) A. R. Utke, R. T. Sanderson, *J. Org. Chem.* **1964**, *29*, 1261–1264; b) S. R. Drake, D. J. Otway, *J. Chem. Soc. Chem. Commun.* **1991**, 517–519; c) S. R. Drake, D. J. Otway, S. P. Perlepes, *Main Group Met. Chem.* **1991**, *14*, 243–256.

[14] a) P. B. Hitchcock, M. F. Lappert, G. A. Lawless, B. Royo, *J. Chem. Soc. Chem. Commun.* **1990**, 1141–1142; b) A. D. Frankland, P. B. Hitchcock, M. F. Lappert, G. A. Lawless, *J. Chem. Soc. Chem. Commun.* **1994**, 2435–2436; c) P. S. Tanner, D. J. Burkey, T. P. Hanusa, *Polyhedron* **1995**, *14*, 331–333; d) A. D. Frankland, M. F. Lappert, *J. Chem. Soc. Dalton Trans.* **1996**, 4151–4152; e) E. D. Brady, T. P. Hanusa, M. Pink, V. G. Young, *Inorg. Chem.* **2000**, *39*, 6028–6037; f) X. He, B. C. Noll, A. Beatty, R. E. Mulvey, K. W. Henderson, *J. Am. Chem. Soc.* **2004**, *126*, 7444–7445.

[15] A. M. Johns, S. C. Chmely, T. P. Hanusa, *Inorg. Chem.* **2009**, *48*, 1380–1384.

[16] S. Harder, S. Müller, E. Huchner, *Organometallics* **2004**, *23*, 178–183.

[17] D. C. Bradley, M. B. Hursthouse, A. A. Ibrahim, K. M. A. Malik, M. Motevalli, R. Möseler, H. Powell, J. D. Runnacles, A. C. Sullivan, *Polyhedron* **1990**, *9*, 2959–2964.

[18] a) M. Westerhausen, *Inorg. Chem.* **1991**, *30*, 96–101; b) M. Westerhausen, J. Greul, H.-D. Hausen, W. Schwarz, *Z. Anorg. Allg. Chem.* **1996**, *622*, 1295–1305; c) M. Westerhausen, M. Hartmann, N. Makropoulos, B. Wieneke, M. Wieneke, W. Schwarz, D. Stalke, *Z. Naturforsch.* **1998**, *53b*, 117–125.

[19] M. M. Gillett-Kunnath, J. G. MacLellan, C. M. Forsyth, P. C. Andrews, G. B. Deacon, K. Ruhlandt-Senge, *Chem. Commun.* **2008**, 4490–4492.

[20] a) M. Westerhausen, *Angew. Chem. Int. Ed.* **2001**, *40*, 2975–2977; *Angew. Chem.* **2001**, *113*, 3063–3065; b) M. Westerhausen, M. Gärtner, R. Fischer, J. Langer, L. Yu, M. Reiher, *Chem. Eur. J.* **2007**, *13*, 6292–6306; c) M. Westerhausen, M. Gärtner, R. Fischer, J. Langer, *Angew. Chem. Int. Ed.* **2007**, *46*, 1950–1956; *Angew. Chem.* **2007**, *119*, 1994–2001; d) M. Westerhausen, *Z. Anorg. Allg. Chem.* **2009**, *635*, 13–32; e) M. Westerhausen, J. Langer, S. Krieck, C. Glock, *Rev. Inorg. Chem.* **2011**, *31*, 143–184; f) M. Westerhausen, J. Langer, S. Krieck, R. Fischer, H. Görls, M. Köhler, *Top. Organomet. Chem.* **2013**, *45*, 29–72; g) M. Westerhausen, A. Koch, H. Görls, S. Krieck, *Chem. Eur. J.* **2017**, *23*, 1456–1483.

[21] a) M. Gärtner, R. Fischer, J. Langer, H. Görls, D. Walther, M. Westerhausen, *Inorg. Chem.* **2007**, *46*, 5118–5124; b) M. Gärtner, H. Görls, M. Westerhausen, *Inorg. Chem.* **2007**, *46*, 7678–7683; c) M. Gärtner, H. Görls, M. Westerhausen, *Dalton Trans.* **2008**, 1574–1582.

[22] C. N. de Bruin-Dickason, G. B. Deacon, C. Jones, P. C. Junk, M. Wiecko, *Eur. J. Inorg. Chem.* **2019**, 1030–1038.

[23] G. J. Moxey, A. J. Blake, W. Lewis, D. L. Kays, *Eur. J. Inorg. Chem.* **2015**, 5892–5902.

[24] S. Krieck, P. Schüler, J. M. Peschel, M. Westerhausen, *Synthesis* **2019**, *51*, 1115–1122.

[25] a) K. Ziegler, H. Froitzheim-Kuhlhorn, K. Hafner, *Chem. Ber.* **1956**, *89*, 434–443; b) E. O. Fischer, G. Stolzle, *Chem. Ber.* **1961**, *94*, 2187–2193; c) R. Zerger, G. Stucky, *J. Organomet. Chem.* **1974**, *80*, 7–17; d) M. Kirilov, G. Petrov, K. Angelov, *J. Organomet. Chem.* **1976**, *113*, 225–232.

[26] M. J. McCormick, R. A. Williams, L. J. Levine, T. P. Hanusa, *Polyhedron* **1988**, *7*, 725–730.

[27] A. P. Borisov, V. D. Makhaev, *Izv. Akad. Nauk Ser. Khim.* **1993**, 377–378.

[28] B. G. Gowenlock, W. E. Lindsell, B. Singh, *J. Chem. Soc. Dalton Trans.* **1978**, 657–664.

[29] M. Gärtner, H. Görls, M. Westerhausen, *Organometallics* **2007**, *26*, 1077–1083.

[30] R. Fischer, J. Langer, S. Krieck, H. Görls, M. Westerhausen, *Organometallics* **2011**, *30*, 1359–1365.

[31] M. J. Harvey, T. P. Hanusa, *Organometallics* **2000**, *19*, 1556–1566.

[32] G. B. Deacon, F. Jaroschik, P. C. Junk, R. P. Kelly, *Organometallics* **2015**, *34*, 2369–2377.

[33] B. Huo, R. Sun, B. Jin, L. Hu, J.-H. Bian, X.-L. Guan, C. Yuan, G. Lu, Y.-B. Wu, *Chem. Commun.* **2021**, *57*, 5806–5809.

[34] E. Beckmann, *Ber. Dtsch. Chem. Ges.* **1905**, *38*, 904–906.

[35] a) H. Gilman, F. Schulze, *J. Am. Chem. Soc.* **1926**, *48*, 2463–2467; b) H. Gilman, L. A. Woods, *J. Am. Chem. Soc.* **1945**, *67*, 520–522; c) D. Bryce-Smith, A. C. Skinner, *J. Chem. Soc.* **1963**, 577–585; d) R. Masthoff, C. Vieroth, *J. Prakt. Chem.* **1968**, *38*, 182–189; e) N. Kawabata, A. Matsumura, S. Yamashita, *Tetrahedron* **1973**, *29*, 1069–1071; f) N. Kawabata, A. Matsumura, S. Yamashita, *J. Org. Chem.* **1973**, *38*, 4268–4270. For a recent review on alkylcalcium compounds see: D. O. Khristolyubov, D. M. Lynbov, A. A. Trifonov, *Russ. Chem. Rev.* **2021**, *90*, 529–565.

[36] F. A. Hart, A. G. Massey, M. Singh Saran, *J. Organomet. Chem.* **1970**, *21*, 147–154.

[37] A. Koch, Q. Dufrois, M. Wirgenings, H. Görls, S. Krieck, M. Etienne, G. Pohnert, M. Westerhausen, *Chem. Eur. J.* **2018**, *24*, 16840–16850.

[38] M. Köhler, A. Koch, H. Görls, M. Westerhausen, *Organometallics* **2016**, *35*, 242–248.

[39] B. M. Wolf, C. Stuhl, C. Maichle-Mössmer, R. Anwander, *J. Am. Chem. Soc.* **2018**, *140*, 2373–2383.

[40] P. E. Eaton, C.-H. Lee, Y. Xiong, *J. Am. Chem. Soc.* **1989**, *111*, 8016–8018.

[41] P. E. Eaton, H. Higuchi, R. Millikan, *Tetrahedron Lett.* **1987**, *28*, 1055–1058.

[42] C. Glock, H. Görls, M. Westerhausen, *Inorg. Chim. Acta* **2011**, *374*, 429–434.

[43] C. Glock, H. Görls, M. Westerhausen, *Inorg. Chem.* **2009**, *48*, 394–399.

[44] a) M. A. Guino-o, A. Torvisco, W. Teng, K. Ruhlandt-Senge, *Inorg. Chim. Acta* **2012**, *389*, 122–130; b) A. N. Selikhov, G. S. Plankin, A. V. Cherkasov, A. S. Shavyrin, E. Louyriac, L. Maron, A. A. Trifonov, *Inorg. Chem.* **2019**, *58*, 5325–5334; c) E. le Coz, H. Roueindeji, V. Dorcet, T. Roisnel, J.-F. Carpentier, Y. Sarazin, *Dalton Trans.* **2019**, *48*, 5500–5504.

[45] A. Torvisco, K. Ruhlandt-Senge, *Inorg. Chem.* **2011**, *50*, 12223–12240.

[46] S. Harder, S. Müller, E. Hübner, *Organometallics* **2004**, *23*, 178–183.

[47] M. Westerhausen, W. Schwarz, *Z. Anorg. Allg. Chem.* **1991**, *604*, 127–140.

[48] J. P. Davin, J.-C. Buffet, T. P. Spaniol, J. Okuda, *Dalton Trans.* **2012**, *41*, 12612–12618.

[49] a) R. Schwarz, M. Pejic, P. Fischer, M. Marinaro, L. Jörissen, M. Wachtler, *Angew. Chem. Int. Ed.* **2016**, *55*, 14958–14962; *Angew. Chem.* **2016**, *128*, 15182–15186. See also: b) P. Schüler, H. Görls, S. Krieck, M. Westerhausen, *Chem. Eur. J.* **2021**, *27*, 15508–15515.

[50] a) X. He, J. F. Allan, B. C. Noll, A. R. Kennedy, K. W. Henderson, *J. Am. Chem. Soc.* **2005**, *127*, 6920–6921; b) X. He, E. Hurley, B. C. Noll, K. W. Henderson, *Organometallics* **2008**, *27*, 3094–3102.

[51] a) R. P. Davis, *Inorg. Chem. Commun.* **2000**, *3*, 13–15; b) X. He, B. C. Noll, A. Beatty, R. E. Mulvey, K. W. Henderson, *J. Am. Chem. Soc.* **2004**, *126*, 7444–7445; c) I. R. Speight, S. C. Chmely, T. P. Hanusa, A. L. Rheingold, *Chem. Commun.* **2019**, *55*, 2202–2205.

[52] D. J. Burkey, E. K. Alexander, T. P. Hanusa, *Organometallics* **1994**, *13*, 2773–2786.

[53] D. Schuhknecht, T. P. Spaniol, Y. Yang, L. Maron, J. Okuda, *Inorg. Chem.* **2020**, *59*, 9406–9415.

[54] P. Schüler, S. Krieck, H. Görls, P. Liebing, M. Westerhausen, *Dalton Trans.* **2022**, *51*, 8461–8471.

[55] M. L. Cole, P. C. Junk, *New J. Chem.* **2005**, *29*, 135–140.

[56] S. Brand, A. Causero, H. Eisen, J. Pahl, J. Langer, S. Harder, *Eur. J. Inorg. Chem.* **2020**, 1728–1735.

[57] A. Causero, G. Ballmann, J. Pahl, H. Zijlstra, C. Färber, S. Harder, *Organometallics* **2016**, *35*, 3350–3360.
[58] M. L. Cole, G. B. Deacon, C. M. Forsyth, K. Konstas, P. C. Junk, *Dalton Trans.* **2006**, 3360–3367.
[59] A. Hinz, *Chem. Eur. J.* **2019**, *25*, 13, 3267–3271.
[60] R. Neufeld, D. Stalke, *Chem. Sci.* **2015**, *6*, 3354–3364.
[61] a) D. Schulze-Sünnighausen, J. Becker, B. Luy, *J. Am. Chem. Soc.* **2014**, *136*, 4, 1242–1245; b) D. Schulze-Sünnighausen, J. Becker, M. R. M. Koos, B. Luy, *J. Magn. Reson.* **2017**, *281*, 151–161.
[62] A. M. Johns, T. S. Ahmed, B. W. Jackson, R. H. Grubbs, R. L. Pederson, *Org. Lett.* **2016**, *18*, 772–775.
[63] R. Hooft: COLLECT, Data Collection Software; Nonius B. V., Netherlands, **1998**.
[64] Z. Otwinowski, W. Minor, in *Methods in Enzymology* (Eds. C. W. Carter, R. M. Sweet), Vol. *276*, part A, Academic Press, San Diego, USA, **1997**, pp 307–326.
[65] SADABS 2.10, Bruker-AXS inc., **2002**, Madison, WI, USA.
[66] Bruker (**2020**) APEX3 Bruker AXS LLC, Madison, WI, USA.
[67] G. M. Sheldrick, *Acta Crystallogr. Sect. A* **2015**, *71*, 3–8.
[68] G. M. Sheldrick, *Acta Crystallogr. Sect. C* **2015**, *71*, 3–8.
[69] A. L. Spek, *Acta Crystallogr. Sect. C* **2015**, *71*, 9–18.
[70] XP, Siemens Analytical X-ray Instruments Inc., Karlsruhe, Germany, **1990**; Madison, WI, USA, **1994**.

Manuscript received: June 20, 2022
Accepted manuscript online: August 1, 2022
Version of record online: August 23, 2022